İSTANBUL TECHNICAL UNIVERSITY ★ INSTITUTE OF SCIENCE AND TECHNOLOGY

THE MECHANISM OF COPPER-CATALYZED CYCLOPROPANATION REACTION : A DFT STUDY

M.Sc. Thesis by

Cihan ÖZEN

Department: Chemistry

Programme: Chemistry

JUNE 2007

İSTANBUL TECHNICAL UNIVERSITY ★ INSTITUTE OF SCIENCE AND TECHNOLOGY

THE MECHANISM OF COPPER-CATALYZED CYCLOPROPANATION REACTION : A DFT STUDY

M.Sc. Thesis by

Cihan ÖZEN

(509051204)

Date of submission: 7 May 2007

Date of defence examination: 13 June 2007

Supervisors (Chairmen): Assist. Prof. Dr. Nurcan TÜZÜN

Members of the Examining Committee: Prof. Dr. Naciye TALINLI

Prof. Dr. Viktorya AVIYENTE (B.U)

JUNE 2007

İSTANBUL TEKNİK ÜNİVERSİTESİ ★ FEN BİLİMLERİ ENSTİTÜSÜ

BAKIR KATALİZÖRLÜ SİKLOPROPANLANMA REAKSİYONUN MEKANİZMASI : BİR DFT ÇALIŞMASI

YÜKSEK LİSANS TEZİ

Cihan ÖZEN

(509051204)

Tezin Enstitüye Verildiği Tarih: 7 Mayıs 2007

Tezin Savunulduğu Tarih: 13 Haziran 2007

Tez Danışmanı: **Yrd. Doç. Dr. Nurcan TÜZÜN**

Diğer Jüri Üyeleri **Prof. Dr. Naciye TALINLI**

Prof. Dr. Viktorya AVIYENTE (B.Ü)

HAZİRAN 2007

ACKNOWLEDGEMENTS

I wish to express my appreciation to Assist. Prof. Dr. Nurcan Tüzün, whose academic expertise, consistent direction and encouragement provided me with the inspiration to undertake and expand upon the research of this study. Also, I am grateful to her for trusting in me, giving me opportunity to approach the thoughts that I just dream of.

I am deeply indebted to my family, who give their ever-present love and devotion, for all the guidance and support.

June, 2007 **Cihan Özen**

CONTENTS

ABBREVIATIONS **v**
LIST OF FIGURES **vi**
LIST OF SCHEMES **vii**
LIST OF SYMBOLS **viii**
SUMMARY **ix**
ÖZET **x**

1. INTRODUCTION **1**
1.1. Cyclopropanes 1
1.2. Computationally Proposed Carbene Formation and Cyclopropanation Mechanisms 6

2. THEORY **10**
2.1. Calculation Methods 10
2.1.1. Ab-initio methods 10
2.1.2. Density functional theory 11
2.1.3. Basis set 14
2.1.4. Intrinsic reaction coordinate 15
2.1.5. Natural bond orbital 15

3. METHODOLOGY **16**

4. RESULTS **17**
4.1. Formation of Copper-Carbene 17
4.1.1. Mechanism 1 19
4.1.1.1 Associative vs dissociative pathways 19
4.1.2. Mechanism 2 25
4.1.3. Mechanism 3 28
4.2. Cyclopropanation Stage 32

5. CONCLUSION **38**

REFERENCES **40**

APPENDIX **45**

BIOGRAPHY **48**

ABBREVIATIONS

B3LYP	: Becke Style Three Parameter Functional in Combination with the Lee-Yang Parr Correlation Functional
BLYP	: Becke's Gradient-Corrected Correlation Functional
DFT	: Density Functional Theory
DMDM	: Dimethyl Diazomalonate
E	: Energy
GTO	: Gaussian Type Orbitals
G03	: Gaussian 03
H	: Hamiltonian Operator
HF	: Hartree-Fock
IRC	: Intrinsic Reaction Coordinate
LDA	: Local Density Approximation
NBO	: Natural Bond Orbital
STO	: Slater Type Orbitals

LIST OF FIGURES

Page No.

Figure 1.1 : Some important synthetic and natural cyclopropanes 1
Figure 1.2 : Carbenes and its types 2
Figure 1.3 : The reactions of carbenes 3
Figure 1.4 : Reactivity of diazo compounds..... 3
Figure 1.5 : Protonation types of diazo compound 4
Figure 1.6 : Possible cyclopropanation mechanism..... 5
Figure 4.1 : Reduced form of the copper(II) catalyst. 17
Figure 4.2 : Trans and cis conformers of DMDM 18
Figure 4.3 : 1:1 and 1:2 catalyst-ethylene complexes 19
Figure 4.4 : Energy differences between associative and dissociative displacements 20
Figure 4.5 : 3-Dimensional geometrical structures 7 and 8..... 21
Figure 4.6 : 3-Dimensional geometrical structure 9 22
Figure 4.7 : 3-Dimensional geometrical structures 10 and 11..... 22
Figure 4.8 : 3-Dimensional geometrical structure copper-carbene complex 12 23
Figure 4.9 : 3-Dimensional geometrical structures 13 and 14. 25
Figure 4.10 : 3-Dimensional geometrical structures 15 and 16 26
Figure 4.11 : 3-Dimensional geometrical structures 17 and 18 28
Figure 4.12 : 3-Dimensional geometrical structure 19 29
Figure 4.13 : 3-Dimensional geometrical structure 20 and 21 30
Figure 4.14 : 3-Dimensional geometrical structures of 22 and 23 32
Figure 4.15 : 3-Dimensional geometrical structures of 24,25 and 26 33
Figure 4.16 : 3-Dimensional geometrical structures of 27a and 27b..... 34
Figure 4.17 : The 4-membered transition state and its IRC result..... 34
Figure 4.18 : 3-Dimensional geometrical structure of 28 36
Figure 4.19 : 3-Dimensional geometrical structure of complexation of double alkene..... 36
Figure 4.20 : Energy differences of structures 10, 11 and 29 37

LIST OF SCHEMES

Page No.

Scheme 1.1 Assisted and Non-assisted metal-carbene formation mechanisms 7
Scheme 1.2 Second mechanism for metal-carbene formation 8
Scheme 1.3 3 and 4 centered cyclopropanation stages..... 9
Scheme 4.1 Mechanism 1 olefin assisted 24
Scheme 4.2 Mechanism 2 olefin non-assisted 27
Scheme 4.3 Mechanism 3. 31
Scheme 4.4 Cyclopropanation stage..... 35

SYMBOLS

$\mathbf{E}$	**:** Energy of the System
$\mathbf{E_b}$	**:** Electrostatic Energy Of Positive Background
$\mathbf{E_c[p]}$	**:** Correlation Functional
$\mathbf{E_c^{VWV}}$	**:** Vosko-Wilk-Nusair Correlation Energy
$\mathbf{\Delta E}$	**:** Difference of Anodic and Catodic Potential
$\mathbf{E_T}$	**:** Kinetic Energy
$\mathbf{E_V}$	**:** Potential Energy
$\mathbf{E_J}$	**:** Coulomb Energy
$\mathbf{E_X[p]}$	**:** Exchange Functional
$\mathbf{E_{XC}}$	**:** Exchange-Correlation Energy
$\mathbf{E_{XC}[p]}$	**:** Exchange-Correlation Energy Functional
$\mathbf{H}$	**:** Hamiltonian Operator
$\mathbf{J[p]}$	**:** Electron-Electron Repulsion
$\mathbf{N}$	**:** Normalization Constant
p	**:** Electron Density
$\mathbf{s}$	**:** Path Length
$T[\rho]$	**:** Kinetic Energy of Interacting Electrons
$T_s[\rho]$	**:** Kinetic Energy of Non-interacting Electrons
$\mathbf{v(r)}$	**:** Potential Imposed by the Nuclei at Position r
$V_{ee}[\rho]$	**:** Interelectronic Interactions
$\mathbf{v}$	**:** Negative Normalized Gradient
$v_{xc}(r)$	**:** Exchange-correlation Potential
$v_{eff}(r)$	**:** External effective Potential
$\rho(r)$	**:** Electron Density Function
$\mathbf{\Psi}$	**:** Wavefunction

THE MECHANISM OF COPPER-CATALYZED CYCLOPROPANATION REACTION: A DFT STUDY

SUMMARY

Cyclopropanes are very important molecules because of their biological activity and serving as a starting compound in various organic reactions. The transition metal-catalyzed decomposition of diazoesters with olefins is the commonest method for synthesizing the cyclopropanes. Among the transition metals, copper is the most convenient one because of its cheapness and efficiency. The mechanism of the copper(I)-catalyzed olefin cyclopropanation reaction with dimethyl diazomalonate has been extensively investigated using DFT method at B3LYP/6-31G(d) level. Ethene has been chosen as olefin to eliminate steric effects and to concentrate solely on the mechanisms. However, carbene formation and its further reaction as an electrophile have ambiguous points since the metal carbene can hardly be observed spectroscopically. In our work, the four different mechanisms have been developed. In each of the mechanisms, a oxygen copper interaction has been observed at the beginning of the reaction which subsequently generates rate-determining dinitrogen extrusion stage in accordance with the literature. Afterthat, cyclopropanation step takes place through a direct carbene addition, metallacyclobutane intermediate formation, or insertion of a second alkene. The direct carbene addition occurs via two pathways; 3-centered and 4-centered pathways. The 3-centered pathway is more preferable over 4-centered pathway. The energetics of possible carbene formation and cyclopropanation mechanisms are demonstrated by our calculations.

BAKIR KATALİZÖRLÜ SİKLOPROPANLANMA REAKSİYONUN MEKANİZMASI : BİR DFT ÇALIŞMASI

ÖZET

Siklopropanlar biyolojik aktiviteleri ve çeşitli organik reaksiyonlarda başlanğıç bileşiği olarak kullanılmasından dolayı önemli bileşiklerdir. Diazoesterlerin olefinlerle geçiş metali katalizörleri altında yaptığı bozunmalar siklopropanların sentezi için en yaygın yöntemdir. Bu bozunma sırasında, karben oluşumu ve karbenin elektrofilik karekteri nedeniyle karben oluşumu sonrası reaksiyon mekanizmasında bazı belirsiz noktalar vardır. Geçiş metalleri arasından bakır, ucuz olması ve verimliligi sayesinde bu alanda en çok kullanılan geçiş metalidir. Bu çalışmada, olefin olarak ethen sistemi sterik etkilerden elimine ederek salt reaksiyon mekanizması araştırmak için seçilmiştir. DFT (Density Functional Theory) kullanılarak siklopropanasyon için olası reaksiyon mekanizmaları B3LYP/6-31G(d) seviyede teorik olarak incelenmiştir ve elde edilen veriler temodinamik açıdan degerlendirilmiştir. Çalışmalarımız sonucunda, dört farklı mekanizma belirlenmiştir. Her bir mekanizmada literatürle uyumlu olarak daha sonradan hız belirliyici dinitrojen çıkışını veren zayıf bir oksijen bakır etileşimi gözlenmiştir. Daha sonra, siklopropanasyon aşaması metallasiklobütan ara ürünü veren direk karben eklenmesi veya ikinci bir alkenin eklenmesi üzerinden gerçekleşir. Direk karben eklenmesi iki şekilde olur; 3-merkezli veya 4-merkezli yollar üzerinden. Teorik hesaplamalara göre, 3-merkezli geçiş yapılı mekanizma 4-merkezli geçiş yapılı mekanizmaya göre daha düşük enerjilidir.Literatür verilerinide göz önüne alarak yaptığımız çalışmalarda, siklopropanasyon için belirli bir mekanizma olmayıp mekanizmanın sistemin yüküne ve diazoesterdeki substute gruba bağlı olduğu görülmüştür. Buna karşın herbir mekanizma için ortak noktaların bulunduğu belirlenmiştir.

1. INTRODUCTION

1.1 Cyclopropanes

Cyclopropanes are a class of organic compounds bearing cyclopropyl group. They occur very frequently as subunits in biologically active natural and synthetic products which make their synthesis attractive among organic chemists. Figure **1.1** demonstrates some important synthetic and natural cyclopropanes [1].

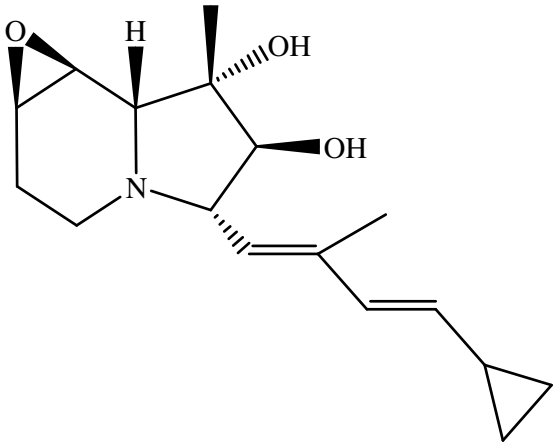

Cyclizidine (indolizidine antibiotic)

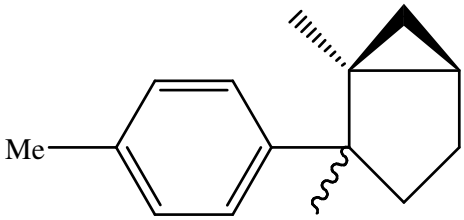

(+)-cyclolaurene

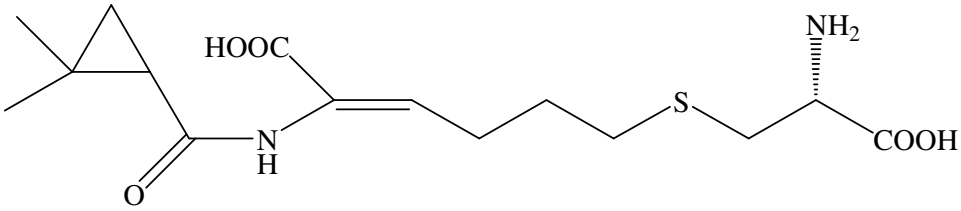

cilastatin

Figure 1.1 : Some Important Synthetic and Natural Cyclopropanes

The commonest method of synthesizing cyclopropanes is via transition metal-catalyzed decomposition of diazoesters with olefins. In this transformation metal-complexed carbenes are produced which further react to form the final cyclopropane product. Several cyclopropane systems with high diastereo- and enantioselectivities have been reported [2-4]. Therefore, carbenes are the key intermediates for cyclopropanation.

Carbenes are highly reactive uncharged intermediates which have two unpaired electrons. If two unpaired electrons are in the same orbital, they are called "singlet carbene" (anti-parallel spins) whereas in "triplet carbenes", the electrons are on different orbitals (Figure **1.2**).

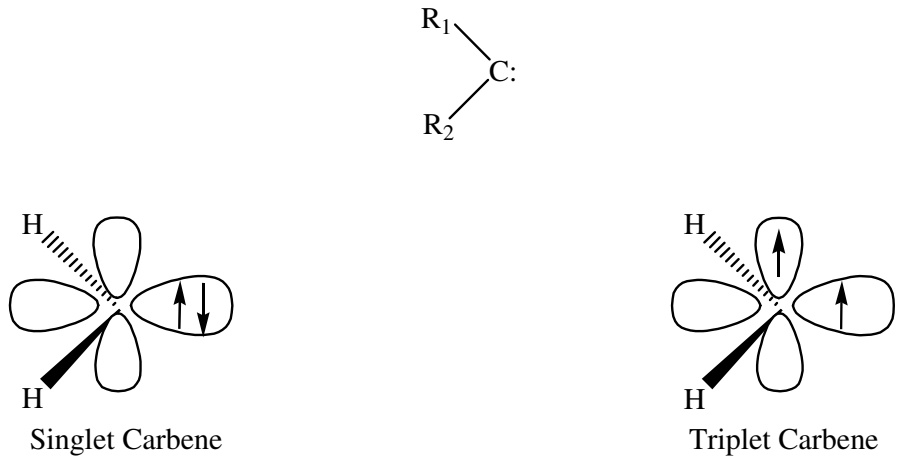

Figure 1.2 : Carbene and Its Types

Singlet and triplet carbenes do not show the same chemical reactivity. Triplet carbenes have diradicalic character and the singlet carbenes may act as electrophile or nucleophile depending on the electron-withdrawing ability of the adjacent groups. Singlet carbenes can be stabilized by transition metal complexes although their naked forms are highly reactive. These complexes are useful in many organic reactions such as cyclopropanation, C-H insertion and nucleophilic attack (Figure **1.3**) [5].

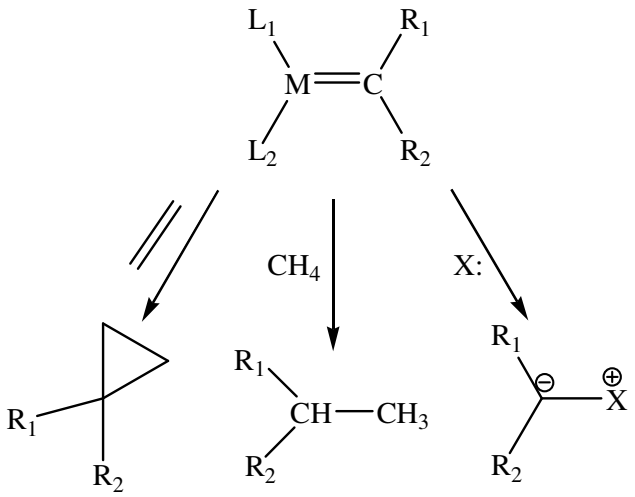

M = Metal L= Ligand X= Nucleophile

Figure 1.3 : The Reactions of Carbenes

In transition metal catalyzed carbene transformation reactions, diazo compounds are essential in order to reduce the metal to form an active catalyst via N_2 elimination. The stability of diazo compounds affects the activity of the catalytically active transition metal compounds. The reactivity of diazocarbonyl compounds depends on the number of carbonyl groups it has. The diazo compounds that have two C=O groups are stated to be less reactive than those with one C=O group. Additionally, substitutents binded to C=O can change the reactivity which can further affect the required reaction conditions (Figure **1.4**) [1].

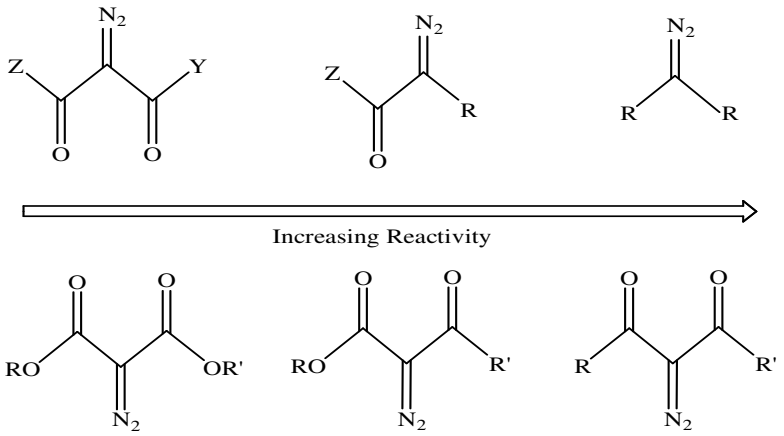

Z and Y = R,OR, NR_2 R = alkyl, aryl, H

Figure 1.4 : Reactivity of Diazo Compounds

Diazocarbonyl compounds are utilized very frequently in catalytic diazo decomposition reactions in which the metal-carbene bond is formed which is used in further transformation. The metal structure (**c**) leads to carbene formation although structures **a** and **b** can be produced as well (Figure **1.5**) [1].

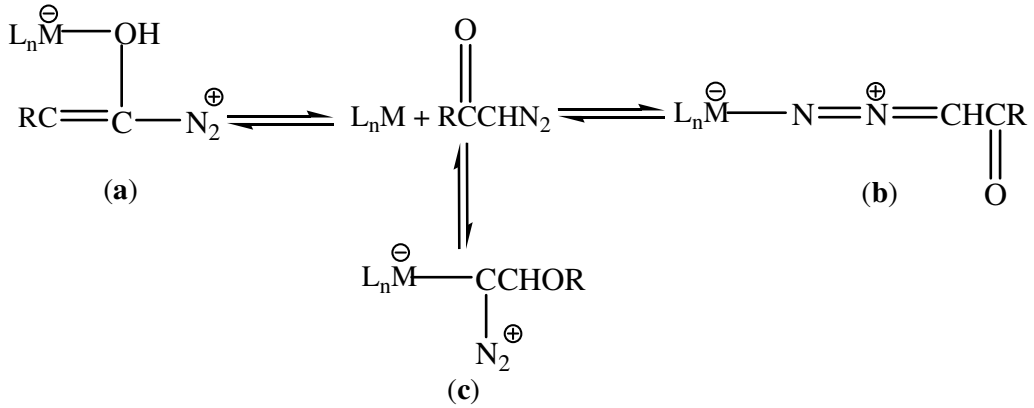

Figure 1.5 : Protonation Types of Diazo Compounds

Metal carbene complexes are rarely observed by spectroscopic methods. Two copper complexes have been detected by Straub and Hofmann using ultra low temperature NMR [6]. Other transition metal carbene species, such as ruthenium and osmium, have been isolated from stoichiometric reactions with diazo esters [7,8].

Among the transition metals, copper-based complexes are more convenient because of their cheapness and efficiency [9] in comparasion with other transition metal catalysts for instances ruthenium-based [10] and rhodium-based [11] complexes. Thus, many researches have concentrated on the use of copper. Historically, Nozaki et al accomplished the first enantioselective reaction using copper salicylaldimine [12]. Then Aratani's asymmetric process of cyclopropanation via Cu based catalysts following Nozaki's work brought metal-mediated transformation of alkene to large-scale industrial production [13]. In spite of the theoretical background, detailed mechanism of cyclopropanation via copper carbene complex is not well known. Actually, there are experimental and theoretical results that are in conflict each other [3,14,15]. However, in these mechanisms, there are some common points. Firstly, entire mechanism consists of two parts. These are metal carbene formation (Scheme **1.1**) and cyclopropanation stages (Scheme **1.2**).

Secondly, it was formerly thought that both Cu(I) and Cu(II) were active catalytic species. According to kinetic data by Kochi et al. Cu(I) is found to be more active species than Cu(II) is. Cu(II) is reduced to Cu(I) by diazo compound [16]. Nowadays, generally, Cu(I) is prepared as "in situ" but little information is known about how it forms the carbene structure [1].

Finally, in cyclopropanation stage, the reaction can be completed by 3 centered or 4 centered pathways. In 3-centered pathway, a direct carbene addition to olefin compound occures. In 4-centered pathway, a metallacyclobutane is formed. It has been stated that the 3-centered pathway is more favorable than the 4-centered [5]. Figure **1.6** shows cyclopropanation stage after carbene formation. Experimental studies on cyclopropanation have also shown some common points about the kinetics of the reaction. It has been obsorved that excess olefin and excess ligand have a decelerating effect on the rate of the reaction. Therefore, a 1:1 catalyst-ethylene proportion is generally considered as the starting species [17].

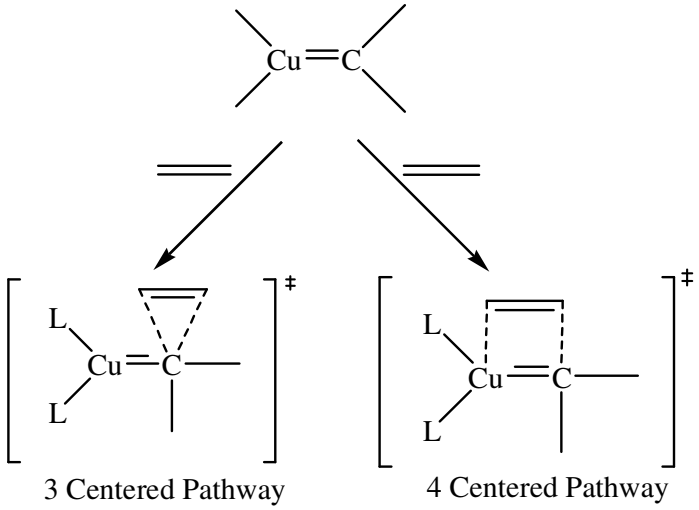

Figure 1.6 : Possible Cyclopropanation Mechanism

In this study, Cu-carbene complex formation and cyclopropanation reactions have been studied starting by ethene as substrate, dimethyl diazomalonate (**DMDM**) as diazo compound and copper(II) acetylacetonate [$Cu(acac)_2$] as transition metal catalyst. This catalyst and the diazo compound have been used in carbene transformation reactions with more complex substrates successfully by Talinli et al. [18]. The main focus of this study is to understand the carbene formation and cyclopropanation mechanisms with this [$Cu(acac)_2$] and DMDM. With this purpose,

all possible mechanisms leading initially to carbene complex then to cyclopropane have been modeled by means of computational chemistry tools. Ethene was chosen as olefin to minimize the steric effects related to substrate and to concentrate solely on the catalyst and the reaction mechanisms. This will enable one to shed light on the catalytic reaction mechanism which works as a black box. Understanding the mechanism in full detail will allow one to modify the factors affecting the reaction in order to govern the reaction and obtain tailor-made products. Moreover, it will be serving as a model study for an ongoing project where larger substrates will be involved in cyclopropanation and some other competing reactions.

1.2 Computationally Proposed Carbene Formation and Cyclopropanation Mechanisms

In the literature, there are some computational studies in which metal-carbene mechanisms are studied in detail. However, these studies demonstrate that the suggested mechanisms depend on the catalyst and the diazo compound. There are mainly two possibilities for metal carbene formation olefin assisted and olefin non-assisted. In the assisted, mechanism olefin molecule is binded to the catalyst until metal-carbene formes. In non-assisted, olefin is detached from catalyst before N_2 extrusion (Scheme **1.1**). In Scheme **1.2**, a third mechanism is proposed based on the results of Fraile et al. on a copper catalyzed cyclopropanation study of an analogous system. In this mechanism, a κO-N chelate complex forms which has been considered a dead-end previously. This chelate complex first coordinates to carbonyl bond which then forms copper-carbene via N_2 loss.

For the cyclopropanation step, the two suggested mechanism are shown in Scheme **1.3**. A three-centered transition state structure leads to a Cu—O complexed structure. The catalyst further leaves the system and cyclopropanation formes. A four-membered ring formation takes place by the reaction of a copper-carbene and ethene. This metallocyclobutane intermediate undergoes another transition state in which the alkene carbons bind to carbene carbon to form cyclopropane product.

In this study, these mechanisms depicted in Scheme **1.1**, Scheme **1.2**, Scheme **1.3** are modelled extensively by DFT B3LYP/6-31G* calculation.

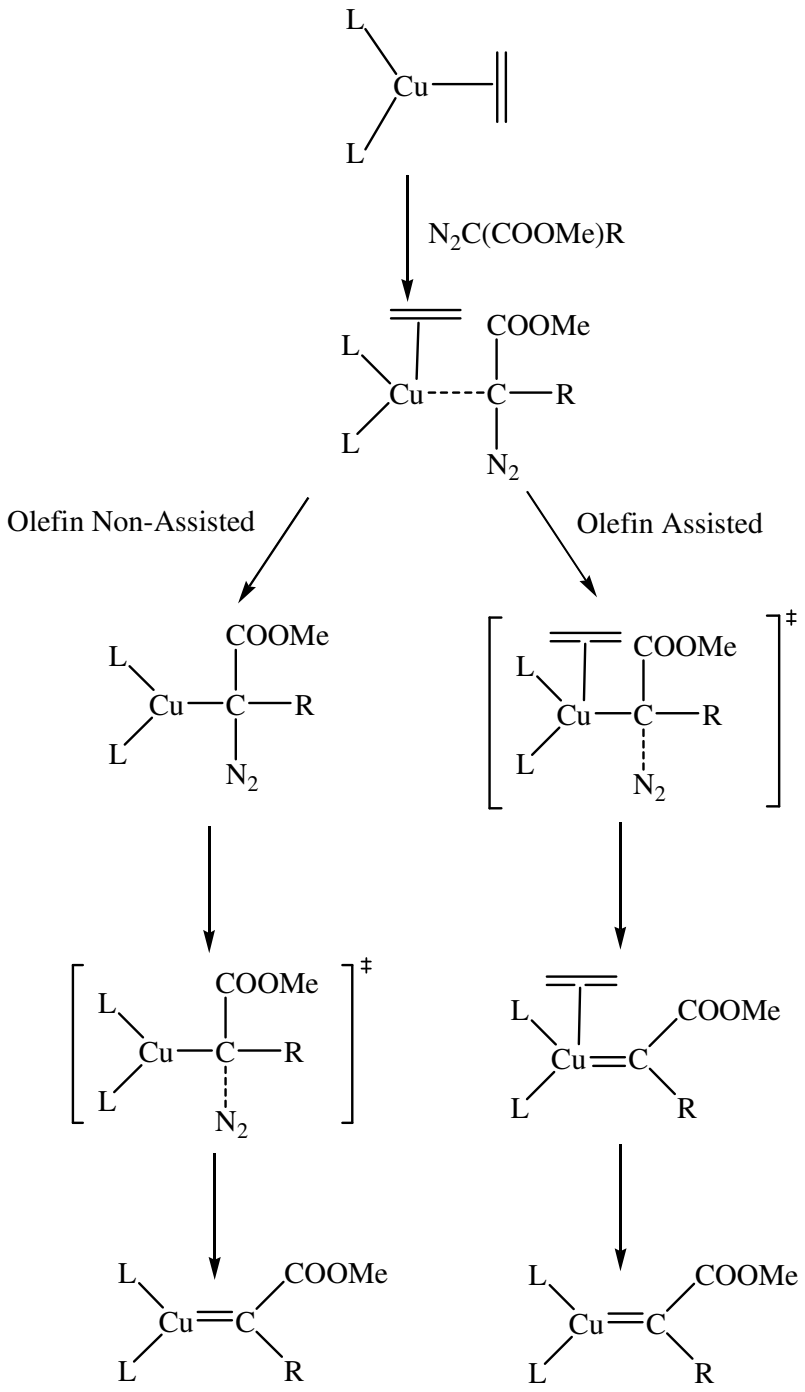

Scheme 1.1 : Assisted and Non-Assisted Metal-Carbene Formation Mechanisms (R = H, COOMe)

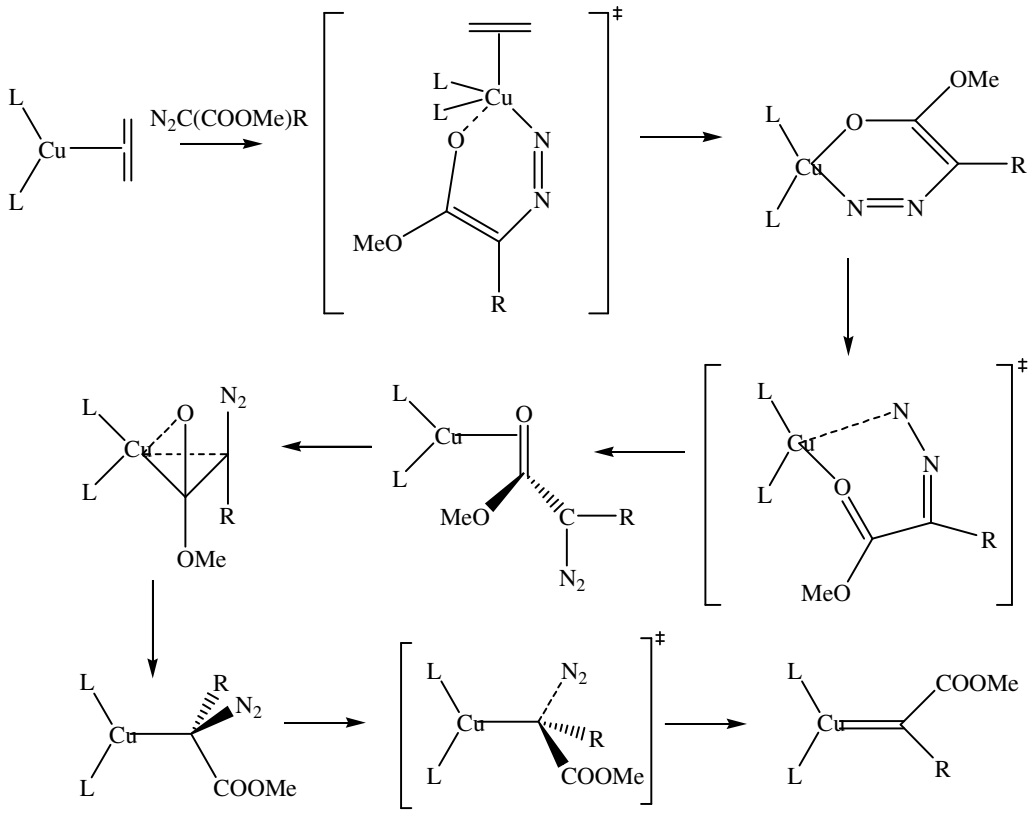

Scheme 1.2 : Second Mechanism for Metal-Carbene Formation (R = H, COOMe)

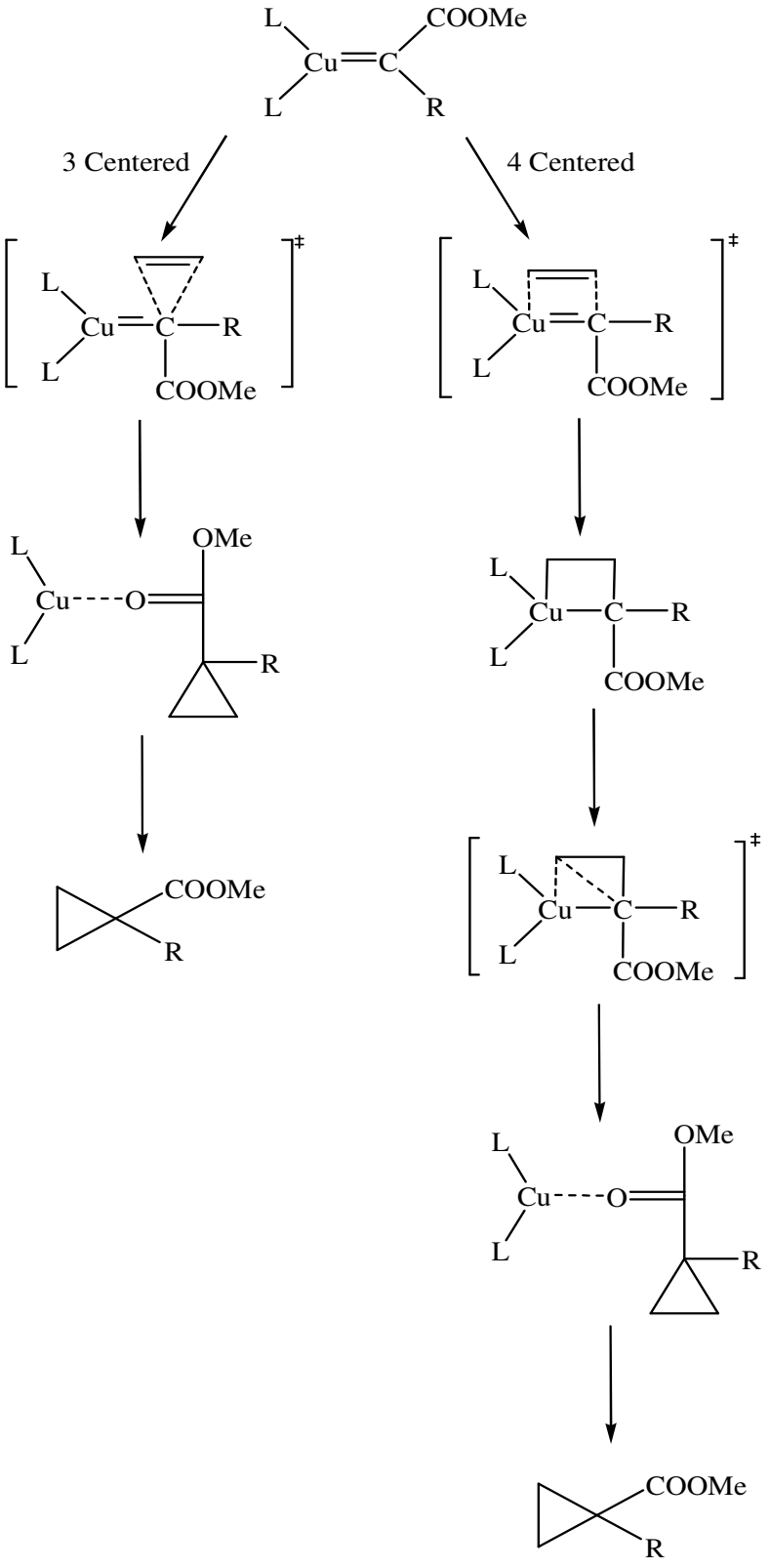

Scheme 1.3 : 3 and 4 Centered Cyclopropanation Stages (R = H, COOMe)

2. THEORY

2.1 Calculation Methods

All computational procedures are based on electronic structure methods which utilizes Schrödinger equation for describing the energy of a system

$$\mathbf{H}\Psi = E\Psi \quad \textbf{(2.1)}$$

where, Ψ is a wavefunction describes the x, y and z spatial coordinates of the particles in the system, E is the energy of the system at that state and **H** is the Hamiltonian operator to derive the kinetic and potential energy of a system. Calculating the exact solution of Schrödinger equation is almost impossible and computationally impractical. Therefore, in electronic structure method, some approximations are used. The mostly encountered three major classes of electronic structure methods are:

- Semi-empirical methods, they use parameters derived from experimental data. Different semi-empirical methods are characterized by their different parameters.
- Ab initio methods, no experimental parameters are used.
- Density functional methods, the total energy of the system only depends on the electron density [19].

2.1.1 Ab-initio Methods

In ab initio method, the Hamiltonian and the wavefunction (Ψ) have been defined, the effective electronic energy can be found by use of the variational method. In the variational method, the best wavefunction is found by minimizing the effective electronic energy with respect to parameters in the wavefunctions [19].

The accuracy of this method depends on chosen wavefunction. However, with increasing molecule size and complexity of wavefunction, ab calculations become more expensive computationally [20].

2.1.2 Density Functional Theory

Density Functional Theory (DFT) [21-24] is a theory in which ground state energy is expressed in terms of electron density. This method was proposed by P. Hohenberg and W. Kohn in 1964 but it contained only virtual functionals. In 1965, Kohn and Sham brought formal functionals based on total electron density. Contrary to Hartree-Fock method [25-27], DFT has smaller computational cost with high accuracy. Although both methods account for the instantaneous interactions of pairs of electrons with opposite spin, DFT methods include the effects of electron correlation (electrons in a molecular system react to one another's motion and attempt to keep out of another's way) while Hartree-Fock calculations see this effect in an average sense (each electron sees and reacts to an averaged electron density).

Density functional methods partition the electronic energy into several terms and compute them separately.

$$E = E_T + E_V + E_J + E_{XC} \qquad \textbf{(2.1.2.1)}$$

E_T is the kinetic energy term, E_V is the potential energy of the nuclear-electron attraction and nuclear-nuclear repulsion term, E_J is the electron-electron repulsion term (also called Coulomb energy), E_{XC} is the exchange-correlation term that includes the remaining part of the electron-electron interactions and it is not known how to calculate exactly.

All the terms except the nuclear-nuclear repulsion, are functions of electron density, $\rho(r)$. E_{XC} can be categorized into exchange and correlation functionals. E_{XC} accounts for the exchange energy arising from the antisymmetry of the quantum mechanical wavefunction and the dynamic correlation in the motions of the individual electrons.

The variational principle determines the ground state energy and electron density in terms of the electron density. Further, the ground state electron density $\rho(r)$ determines the external potential, $v(r)$ and variationally determines the ground state properties of the system of interest.

The electronic energy can be expressed as a functional of the electron density:

$$E[\rho] = \int v(r)\rho(r)dr + T[\rho] + V_{ee}[\rho] \qquad \textbf{(2.1.2.2)}$$

where $T[\rho]$ is the kinetic energy of interacting electrons and $V_{ee}[\rho]$ is the interelectronic interactions.

The electronic energy may be written in the form of Kohn-Sham approach**.**

$$E[\rho] = \int v(r)\rho(r)dr + T_s[\rho] + J[\rho] + E_{xc}[\rho] \qquad \textbf{(2.1.2.3)}$$

This is based upon an orbital density description that removes the necessity of knowing the exact form of $T[\rho]$. Kohn-Sham proposed focusing on the kinetic energy of non-interacting system of electrons $T_s[\rho]$, as a functional of a set of single particle orbitals that give exact density.

$$T_s[\rho] = \sum_{i=1}^{N} \langle \Psi_i | -\frac{1}{2}\nabla^2 | \Psi_i \rangle \qquad \textbf{(2.1.2.4)}$$

$J[\rho]$ represents the electron-electron repulsion (Coulomb energy), and $E_{xc}[\rho]$ is the exchange-correlation energy functional with its functional derivative called the exchange-correlation potential, $v_{xc}(r)$.

$$E_{xc}[\rho] = T[\rho] - T_s[\rho] + V_{ee}[\rho] - J[\rho] \qquad \textbf{(2.1.2.5)}$$

$$v_{xc}(r) = \frac{\partial E_{xc}[\rho]}{\partial \rho(r)} \qquad \textbf{(2.1.2.6)}$$

$E_{xc}[\rho]$ is divided into two parts, namely an exchange functional, $E_x[\rho]$ and a correlation functional, $E_c[\rho]$.

$$E_{xc}[\rho] = E_x[\rho] + E_c[\rho] \qquad \textbf{(2.1.2.7)}$$

$E_x[\rho]$ and $E_c[\rho]$ functionals can be both local and gradient-corrected functionals. Local or gradient-corrected functionals are called traditional functionals. Local functionals depend only on electron density ρ, while gradient-corrected fuctionals depend on both ρ and its gradient, $\Delta\rho$.

A system of non-interacting electrons moving in an external effective potential $v_{eff}(r)$ is shown as;

$$v_{eff}(r) = v(r) + \frac{\partial J[\rho]}{\partial \rho(r)} + \frac{\partial E_{xc}[\rho]}{\partial \rho(r)} = v(r) + \int \frac{\rho(r')}{|r - r'|} dr' + v_{xc}(r) \qquad \textbf{(2.1.2.8)}$$

Now, an equation very similar to the Schrödinger Equation exists.

$$\left[-\frac{1}{2}\nabla^2 + v_{eff}(r) \right] \Psi_i = \varepsilon_i \Psi_i \qquad \textbf{(2.1.2.9)}$$

(2.1.2.3), (2.1.2.4), (2.1.2.5), (2.1.2.6), (2.1.2.7), (2.1.2.8) are Kohn-Sham Equations.

In order to evaluate the exchange-correlation functional some approximations are made. The first one is the local density approximation (LDA). It is based upon a model of uniform electron gas. In the uniform electron gas model, a large number of electrons uniformly spread out in a cube where there is a uniform distribution of the positive charge to make the system neutral. It assumes that the charge density varies slowly throughout the molecule so that a localized region of the molecule behaves like a uniform electron gas The energy expression is:

$$E[\rho] = T_s[\rho] + \int \rho(r) v(r) dr + J[\rho] + E_{xc}[\rho] + E_b \qquad \textbf{(2.1.2.10)}$$

where E_b is the electrostatic energy of the positive background. Since the positive charge density is the negative to the electron density the equation reduces to:

$$E[\rho] = T_s[\rho] + E_{xc}[\rho] = T_s[\rho] + E_x[\rho] + E_c[\rho] \qquad \textbf{(2.1.2.11)}$$

The exchange functional is given by:

$$E_x[\rho] = -C_x \int \rho(r)^{4/3} dr \qquad \textbf{(2.1.2.12)}$$

C_x=0.7386, this form was developed to reproduce the exchange energy of a uniform electron gas.

DFT methods are defined by pairing an exchange functional with a correlation functional and can be named as traditional or hybrid functionals. Hybrid functionals include exact term in the exchange functional, whereas traditional functionals do not.

BLYP (Becke's gradient-corrected exchange functional with Lee-Yang-Parr's gradient-corrected correlation functional) method is a traditional functional whereas, B3LYP (Becke style three parameter functional in combination with the Lee-Yang-Parr correlation functional) method [28], the linear combination of LDA, B88, exact and LYP functionals, is a hybrid functional:

$$E_{xc} = E_{xc}^{LDA} + a_0(E_x^{exact} - E_x^{LDA}) + a_x \Delta E_x^{B88} + a_c \Delta E_c^{non-local} \quad \textbf{(2.1.2.13)}$$

where ΔE_x^{B88} is the Becke's gradient correction, i.e. the second term at the right hand side of the equation (2.1.3.11) and the correction to the correlation ($\Delta E_c^{non-local}$) is provided by the Lee-Yang-Parr functional. But, LYP includes both local and non-local terms, then the correlation functional used is actually: $a_c E_c^{LYP} + (1 - a_c) E_c^{VWN}$ where E_c^{VWN} is the Vosko-Wilk-Nusair correlation energy. The parameters are specified by Becke by fitting the atomization energies, ionization potentials, proton affinities and first row atomic energies in the molecule set, a0=0.20, ax=0.72 and ac=0.81. Hybrid functionals have proven to be superior to the traditional functionals [19].

2.1.3 Basis Sets

A basis set is a serie of basis functions which is used to expressed molecular orbitals. The molecular orbitals are emphasized as a linear combination of basis funtions which are pre-defined one-electron atomic functions. The basis functions are categorized into two classes, Slater Type Orbitals (STO) and Gaussian Type Orbitals (GTO). Slater Type Orbitals have the functional form

$$\Theta_{abc}(x,y,z) = N x^a y^b z^c e^{-\zeta r} \quad \textbf{(2.1.3.1)}$$

N is the normalization constant, a, b and c are angular momentum (L= a+b+c). Gaussian type orbitals can be written as

$$\Theta_{abc}(x,y,z) = N x^a y^b z^c e^{-\zeta r^2} \quad \textbf{(2.1.3.2)}$$

GTOs are preferable over STOs because of the computational efficiency although STOs are more accurate. Among the types of the basis sets (minimal basis sets, split valence basis sets, polarized basis sets, high angular momentum basis sets) the most popular one is the split valence basis set which is developed by Pople and his group termed as 3-21G, 4-31G, 6-31G. Split valence basis sets allow orbitals to change size

not the shape. Polarized basis sets remove this limitation by adding orbitals with angular momentum beyond the ground state configuration for each atom. In this study 6-31G*, also known as 6-31G(d) polarization basis set is used where d functions are added to heavy atoms [19,29].

2.1.4 Intrinsic Reaction Coordinate

Intrinsic Reaction Coordinate (IRC) [30,31] is a minimum energy reaction path on a potential energy surface in mass-weighted coordinates, connecting reactants to products via the transition state [32]. When a transition state is optimized with an imaginary frequency, it must be confirmed that it is the correct transition state. By making IRC calculations. The IRC path is defined by the differential equation

$$\frac{d\mathbf{x}}{ds} = -\frac{\mathbf{g}}{|\mathbf{g}|} = \mathbf{v} \qquad \textbf{(2.1.4.1)}$$

Where x is the mass-weighted coordinates, s is the path length and v is the negative normalized gradient [29].

2.1.5 Natural Bond Orbital

Natural Bond Orbital (NBO) [33-40] analysis is the diagonalization of first-order density matrix which is used to define character of bonds and orbitals. Let A, B and C are the atoms of a molecule. The density matrix can be written in terms of blocks of basis functions belonging to a specific centre as

$$D = \begin{pmatrix} D^{AA} & D^{AB} & D^{AC} & \dots \\ D^{AB} & D^{BB} & D^{BC} & \dots \\ D^{AC} & D^{BC} & D^{CC} & \dots \\ .. & .. & .. & \dots \end{pmatrix} \qquad \textbf{(2.1.5.1)}$$

NBO for A can be defined as diagonalization of the D^{AA} block. The same process is valid for B by D^{BB} block and C by D^{CC} block. NBOs are not orthogonal and orbital occupation numbers are not the total number of electrons [29].

3. METHODOLOGY

In the context of this study, all possible reaction mechanisms will be modeled and discussed in terms of relative energies obtained from quantum mechanical calculations. All the intermediates, transition state structures are modeled by the following methodology. DFT method employing the B3LYP functional with the 6-31G* basis set has been used to carry out the full optimization of the compounds of interest in the gas phase with the G03 package [41]. The DFT methodology with B3LYP functional has been shown to give reliable results with Cu catalyzed carbene transformation and cyclopropanation reactions by Straub et al. [14] and Fraile et al. [13]. This methodology have also been used successfully by in other carbene transformation reactions with ruthenium and palladium catalysis [42,43].

The stationary points were analyzed by vibrational frequency calculations. The transition states were verified to be saddle points by one imaginary frequency belonging to the reaction coordinate. IRC calculations have been performed on transition states to obtain minima on both sides. The structures obtained from IRC calculations were further optimized for their local minima. The electronic energies were corrected by non-scaled zero point energies and Gibbs free energies were calculated at the 298 K. The activation energies, free energies of activation, entropies of activation, the energies of reaction and free energies of reaction are discussed throughout the study.

NBO analysis has been carried out on some structures in order to investigate the stabilizing donor-acceptor interactions and the nature of the Cu-C bonds in some selected structures.

The energetics of some selected structures were further improved by using higher level of calculations, by the B3LYP functional at 6-311+G(d,p) basis set. This basis set has been stated to produce successful results in treating diazo decomposition in cyclopropanation reaction of via Cu based cataylst [14].

4. RESULTS

4.1 Formation of Copper-Carbene

In several studies of Talinli and Anaç et al. [18], $Cu(acac)_2$ and DMDM have been used successfully as catalyst and diazo compound respectively, in carbene transformation reactions in which cyclopropane is one of the product kinds.

A model study of cyclopropanation with ethene as substrate, $[Cu(acac)_2]$ as catalyst and DMDM diazo compound is designed in order to understand the carbene formation and cyclopropanation steps. With this aim, all the possible reaction mechanisms that have been proposed will be tested with quantum mechanical calculations.

Firstly, the reactant molecules have been optimized for their global minimum structures with the B3LYP/6-31G(d) basis set. As explained in the introduction part, Cu(I) form of the metal has been stated as the active catalyst. The reduced form of $[Cu(acac)_2]$(**1**) (Figure **4.1**)has a planar structure with its ligand. The Cu-O distances are 1.807 Å and the O-Cu-O angle is 126.28°

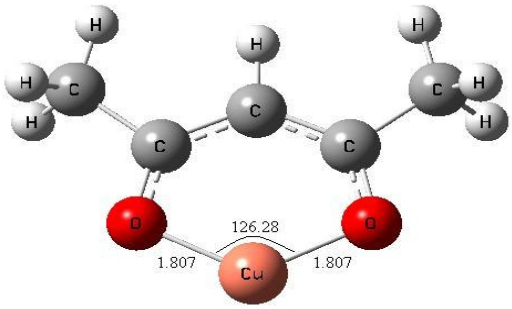

Figure 4.1 : Reduced Form of the Copper(II) Catalyst (**1**)

The diazo compound, dimethyl diazomalonate, has a planar structure due to extended conjugation through C=O and N≡N moieties, as shown in Figure **4.2**. The dimethyl

diazo compound can have cis or trans orientation of C=O groups with respect to each other. In one of the two cis conformations, C=O groups are syn with the diazo group (cis **2**), whereas in the other one they are in anti orientation with the diazo (cis **1**).

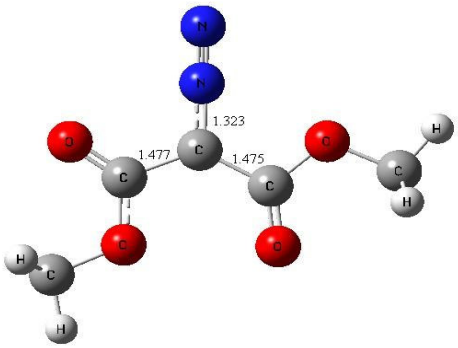

Structure **2 (Trans)**

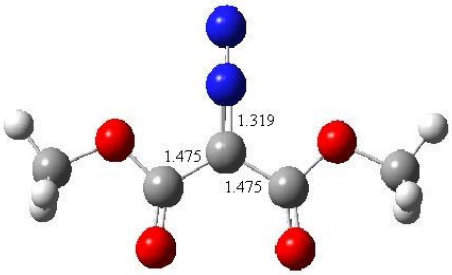

Structure **3 (Cis 1)**

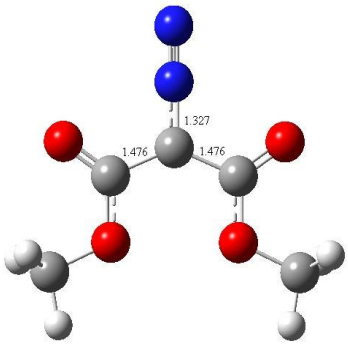

Structure **4 (Cis 2)**

Figure 4.2 : Trans and Cis Conformers of **DMDM**

Gibbs free energies of these three conformers are very close to each other. Among them, the structure **2** conformation has the lowest energy over structure **3** and structure **4** by 0.2 and 0.7 kcal/mol, respectively. Hence, trans conformation was chosen as diazo compound throughout the mechanisms. However, conformation difference revealed no effect on the mechanism.

4.1.1 Mechanism 1

According to kinetic studies, olefin excess retards the rate of cyclopropanation reaction because of the pre-equilibrium [17] involving the catalyst-olefin complexes where catalyst-olefin stoichiometry of 1:1 and 1:2 are possible. Thus 1:1 and 1:2 complexes are calculated in order to compare their thermodynamic stabilities.

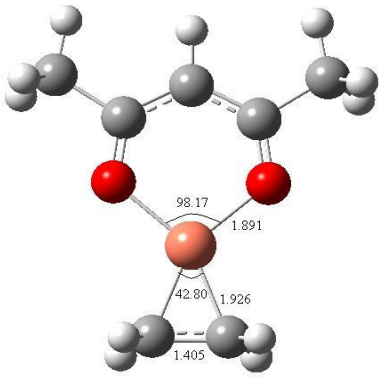

Structure **5**

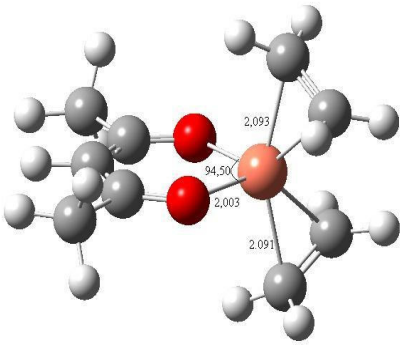

Structure **6**

Figure 4.3 : 1:1 and 1:2 Catalyst-Ethylene Complexes

Structure **5** (Figure **4.3**) has a planar geometry and both of the Cu-C bond lengths are the same with a distance of 1.926 Å. Compared to the naked catalyst, O-Cu-O angle becomes smaller and the Cu-O distance increases as a result of electron-rich ethene satisfying the electron deficiency of copper. On the other hand, in structure **6** (Figure **4.3**), copper is coordinated to two ethene molecules and has the tetrahedral geometry. Thermodynamically, Gibbs free energies favor structure **5** by 9.23 kcal/mol. Thus, it is selected as the reference point for the whole mechanisms. Having determined the starting compound, the structures from suggested mechanisms (Schemes **1.1**, **1.2**, and **1.3**) are calculated by DFT B3LYP/6-31G(d) basis set.

4.1.1.1 Associative vs Dissociative Pathways

The transformation of catalyst-ethylene species to catalyst-diazo compound can occur via two pathways; associative and dissociative displacements [14,15]. In the dissociative displacement, naked catalyst binds to the diazo compound whereas in the associative displacement, it is the catalyst-ethylene complex that binds to the diazo compound. In this system, the calculations indicate that the dissociative displacement requires a higher energy of 38.79 kcal/mol than the associative path. Figure **4.4**

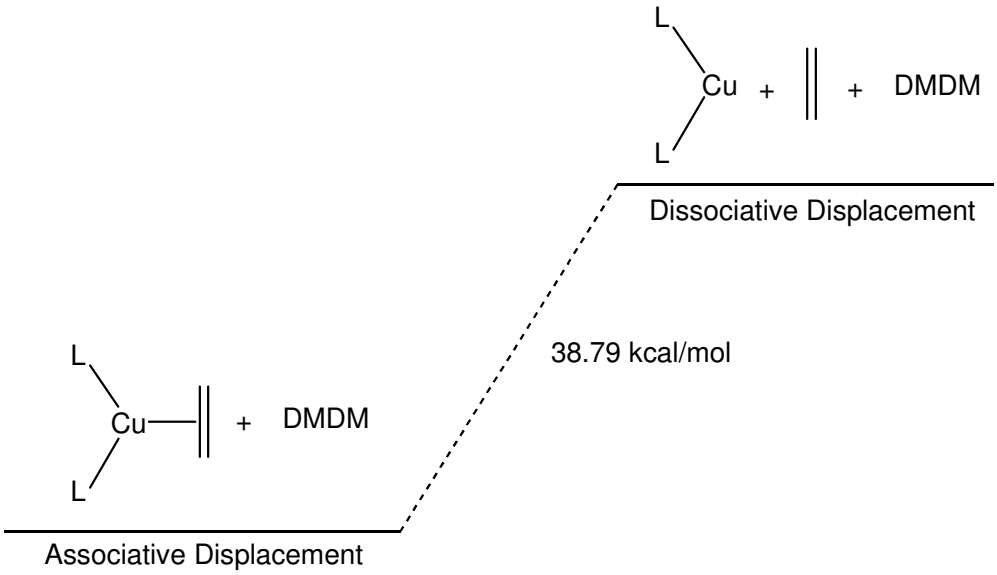

Figure 4.4 : Energy Differences Between Associative and Dissociative Displacements

Thus, it is expected that the associative path is favored over the dissociative. This is in accordance with the results of Fraile et al. [13] on with Cu(I) catalyst where dissociative displacement required 34.2 kcal/mol higher energy than associative displacement in their system. Straub et al. [15] have also found associative displacement a more feasible pathway than the dissociative in their system.

In the associative displacement, κN (**7**), κO (**8**) and κC coordinated complexes are possible, however κC complex could not be obtained as a local minimum. Although higher basis sets (6-311G(d,p) , 6-311+G(d,p)), different method (HF method) and different functionals are tried, none of them were successfull. All attempts shifted to κO complex. In the literature, κC complexes are found in cationic systems [14,15]. Additionally, coordination strength of ligands to cationic metal fragment is greater than neutral system is because positive charge is stabilized by the larger molecular volume [15].

Both κO and κN complexes (Figure **4.5**) have similar energies such that κO is favored by only 0.8 kcal/mol as compared to κN.

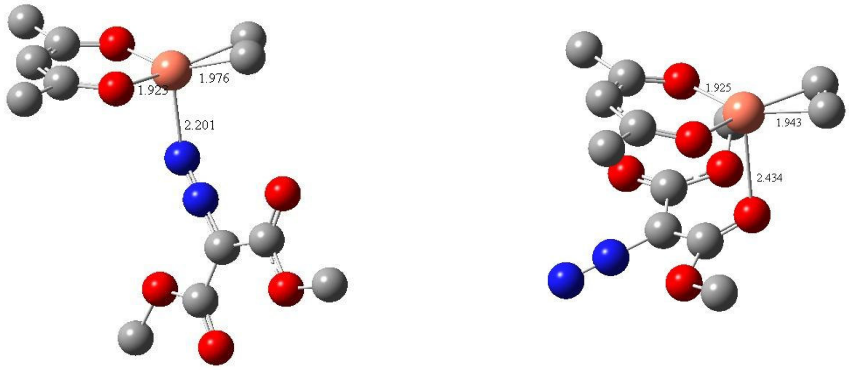

κN (**7**) κO (**8**)

Figure 4.5 : 3-Dimensional Geometrical Structures of **7** and **8** (B3LYP/6-31G*)

Conversion from κN to κO is feasible because of the small free energy difference between them and expected to be almost barrierless since all attempts for a transition state shifted to κO .

Carbene formation mechanism is divided into two parts; olefin assisted and olefin non-assisted pathways. Firstly, olefin assisted part was taken into account (Scheme **1.1**). Structure **8** undergoes an N_2 extrusion step in accordance with Fraile et al. assisted mechanism. This transition state **9** (Figure **4.6**) requires 24.18 kcal/mol for activation and it has the highest Gibbs free energy value on olefin assisted mechanism. Hence, this is the rate determining step. There is a great geometrical change from **8** to **9** because weakening of N-C bond renders C atom a highly reactive center to bind to copper. This is reflected in high activation barrier as well. The electronic energy difference between reactant (**8**) and transition state (**9**) is 26.75 kcal/mol which decreases by only small amount by the negative contribution of entropy. The Cu-O distance is 2.434 Å, which indicates that structure **8** is a pre-reactive complex. The C-N distance in **8** increases from 1.323 Å to 1.880 Å in **9**. The Cu-O distances in its ligand are 1.926 Å, which extend to 2.017 Å and 1.997 Å in the transition state. The Cu-C_{alkene} distances are 1.940 Å and 1.944 Å in structure **8**. As with other atoms coordinating to Cu, their distances also increase to 2.052 and 2.070 Å, respectively. Cu also undergoes pyramidalization as it proceed to N_2 extrusion transition state. Thus, these geometrical changes indicate that as the system goes through N_2 extrusion, coordination number of Cu is increasing. Hence, the bonds it makes with its ligands, substrate and the diazo compound are getting weaker. Structure **8** was also verified by performing IRC calculations on transition state **9**,

which followed the reaction coordinate to **8** as reactant and **10** as product of transition state **9**.

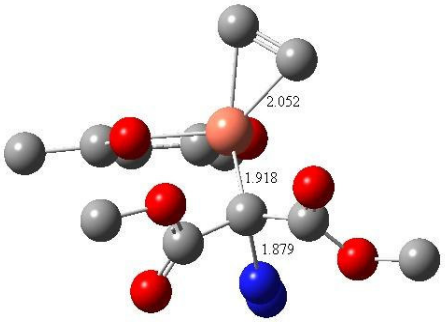

Figure 4.6 : 3-Dimensional Geometrical Structure of **9** (N_2 Extrusion Transition State) (B3LYP/6-31G*)

The N_2 extrusion reaction is endothermic by 24.18 kcal/mol. Structure **10** (Figure **4.7**) was formed as a intermediate with 5.81 kcal/mol of Gibbs free energy relative to starting compound. Although Fraile et al. proposed an alkene loss without a transition state to form metal-carbene molecule, the calculations indicated that a transition state structure **11** (Figure **4.7**) is occured during the metal-carbene formation with a small Gibbs free energy barrier by 2.01 kcal/mol. In alkene loss reaction, The Cu center is 28.0° out of the plane of O_{ligang}- O_{ligang}-C_{DMDM} plane at the reactant (**10**) which decreases to 23.2° in the transition state (**11**) and finally becomes planar at the end of reaction.

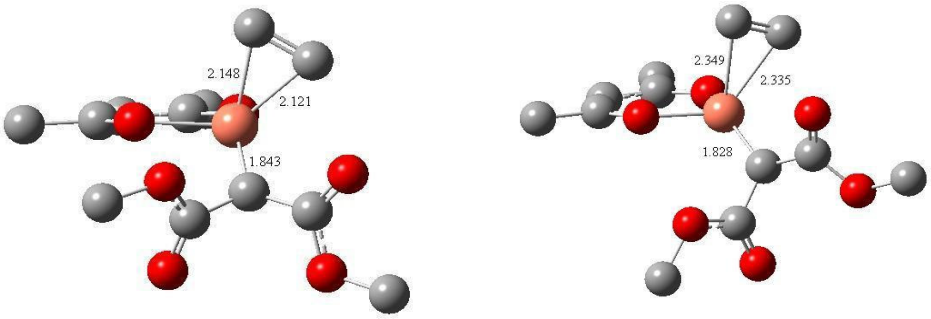

Figure 4.7 : 3-Dimensional Geometrical Structures of **10** and **11** (B3LYP/6-31G*)

Copper-carbene complex structure **12** (Figure **4.8**) is formed after alkene loss transition state with -4.57 kcal/mol of relative Gibbs free energy. This structure is another common intermediate in both assisted and non-assisted pathways. The length

of Cu-C bond is 1.770 Å which is shorter than the experimental data for copper-carbene complexes (1.868 – 1.888 Å) [44]. This bond was 1.843 Å in **10** which shortened to 1.828 Å in the transition state **11** due to increased coordination to carbene carbon. As expected, the carbonyl groups take almost perpendicular position (dihedral angle is 76.48°) with respect to copper-carbene species because of the back-donation from one of the d orbitals of Cu to empty p orbital of the carbene carbon [42]. Additionally, O-Cu-C angles are different by 10° from each other. This indicates that copper-carbene bond deviates from symmetry axis of the naked catalyst in accordance with the work of Fraile et al. on some other Cu(I) catalysts [14]. According to NBO analysis, copper-carbene contains a true copper carbon double bond. The π bond is situated mainly at copper atom 66.74% with 7.33% s and 92.08% d character. For the σ bond, the contribution of carbon atom is 85.92% with 24.58% s and 75.42% p character and of copper atom is 18.08% with 85.39% s and 14.07% d charater. As a result, the carbene carbon is sp^2 hybridized and copper-carbene complex is a kind of Fischer carbene (singlet carbene).

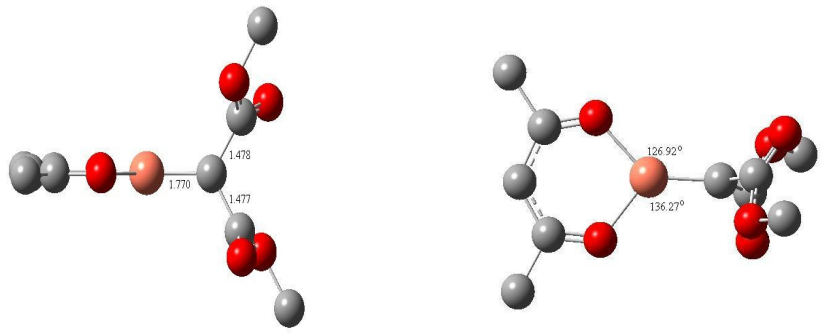

Figure 4.8 : 3-Dimensional Geometrical Structure of Copper-Carbene Complex **12** (B3LYP/6-31G*)

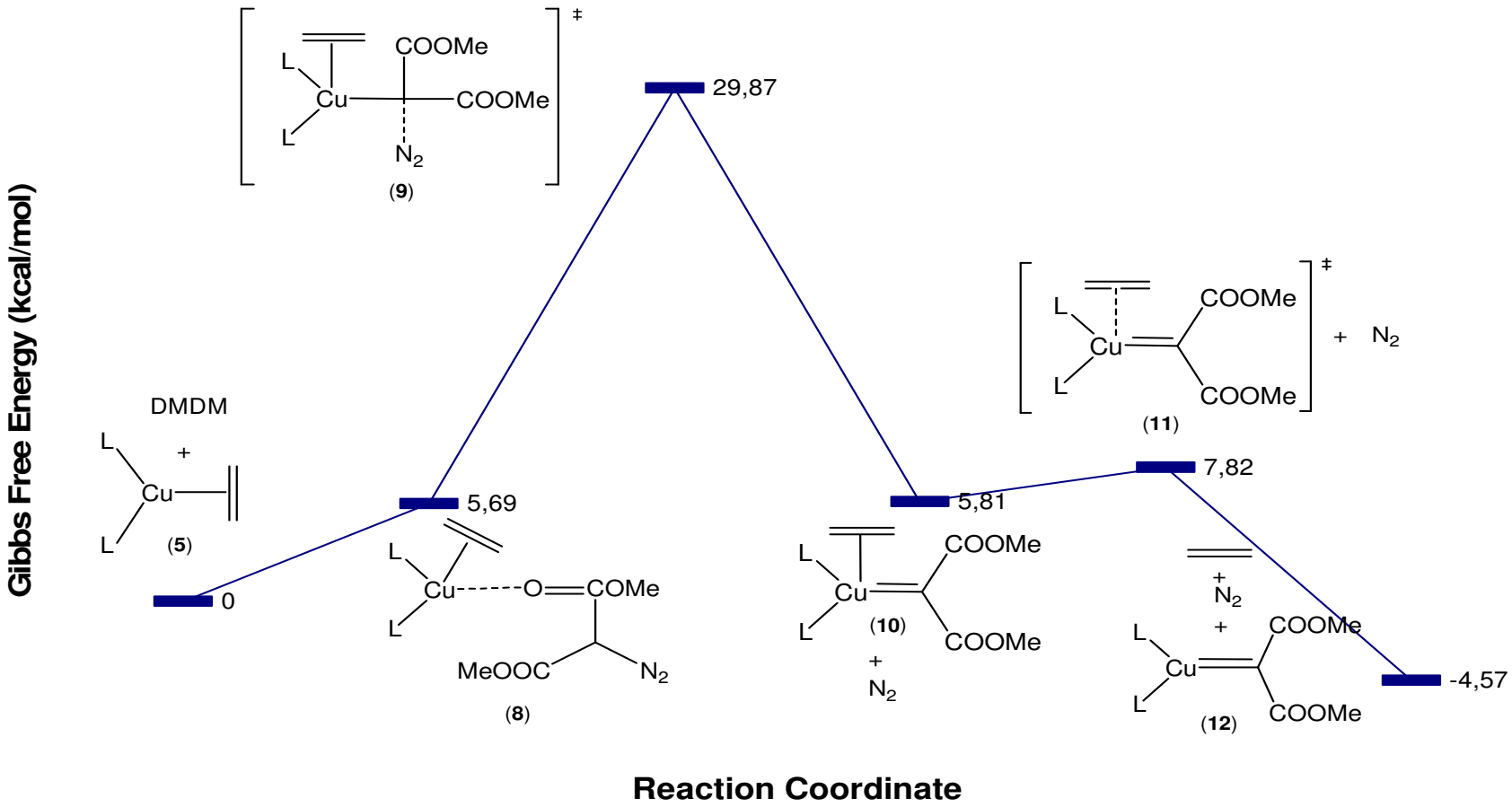

Scheme 4.1 : Mechanism **1**: Olefin Assisted

4.1.2 Mechanism 2

This mechanism differs from olefin assisted mechanism mainly in N_2 and alkene extrusion steps (Scheme **4.2**). Firstly, the pathway starts by the formation of κO copper-complex. When the complex (**8**) detaches alkene group copper coordinates to carbonyl double bond to complete its coordination (**13**) (Figure **4.9**). In the literature, no transition state structure is suggested for alkene loss from the κC copper-complex. A transition state could not be located from the κO copper-complex (**8**) to form **13**. Although a structure could not be located for this transition, a barrier of at least 12.02 kcal/mol (17.71-5.69) is expected by considering the relative Gibbs free energies of **8** and **13**. After structure **13**, Cu loses its coordination to carbonyl bond and binds to carbene carbon by going through transition state **14** (Figure **4.9**).

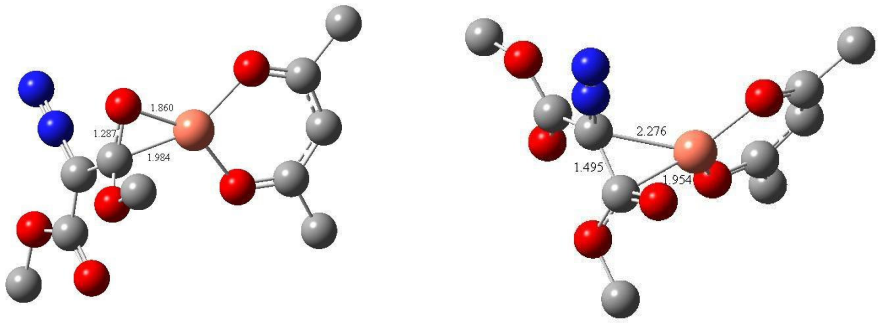

Figure 4.9 : 3-Dimensional Geometrical Structures of **13** and **14** (B3LYP/6-31G*)

Structure **15** (Figure **4.10**) is formed from structure **14** as suggested by Fraile et al. and Gibbs free energy is decreased by 5.52 kcal/mol. In this structure, Cu is in very close vicinity of carbonyl carbon (2.006 Å) so that Cu compansates its coordination deficiency. After structure **15**, N_2 extrusion step takes place as expected. The transition state structure **16** (Figure **4.10**) has the highest Gibbs free energy value on the olefin non-assisted mechanism and this step is rate-determining as in mechanism **1**. Additionally, the olefin non-assisted transition state (**16**) is slightly lower in energy than the olefin assisted one (**9**). The barrier is lower because the reactant (**15**) does not undergo a dramatic change in geometry as it loses N_2 because Cu does not pyramidalize as in olefin assisted N_2 extrusion. The structure **15** has a Cu-C bond length of 1.939 Å which undergoes a shortening during N_2 loss (1.835 Å in **16**) due

to increased coordination between Cu and carbene C. N_2 loss results in copper-carbene structure (**12**) that is discussed in mechanism **1**.

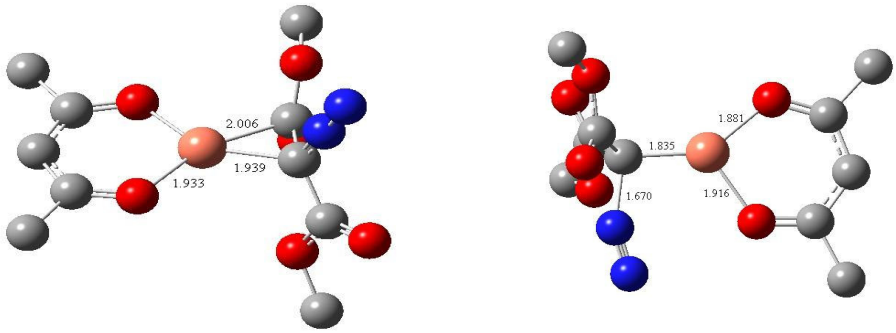

Figure 4.10 : 3-Dimensional Geometrical Structures of **15** and **16** (B3LYP/6-31G*)

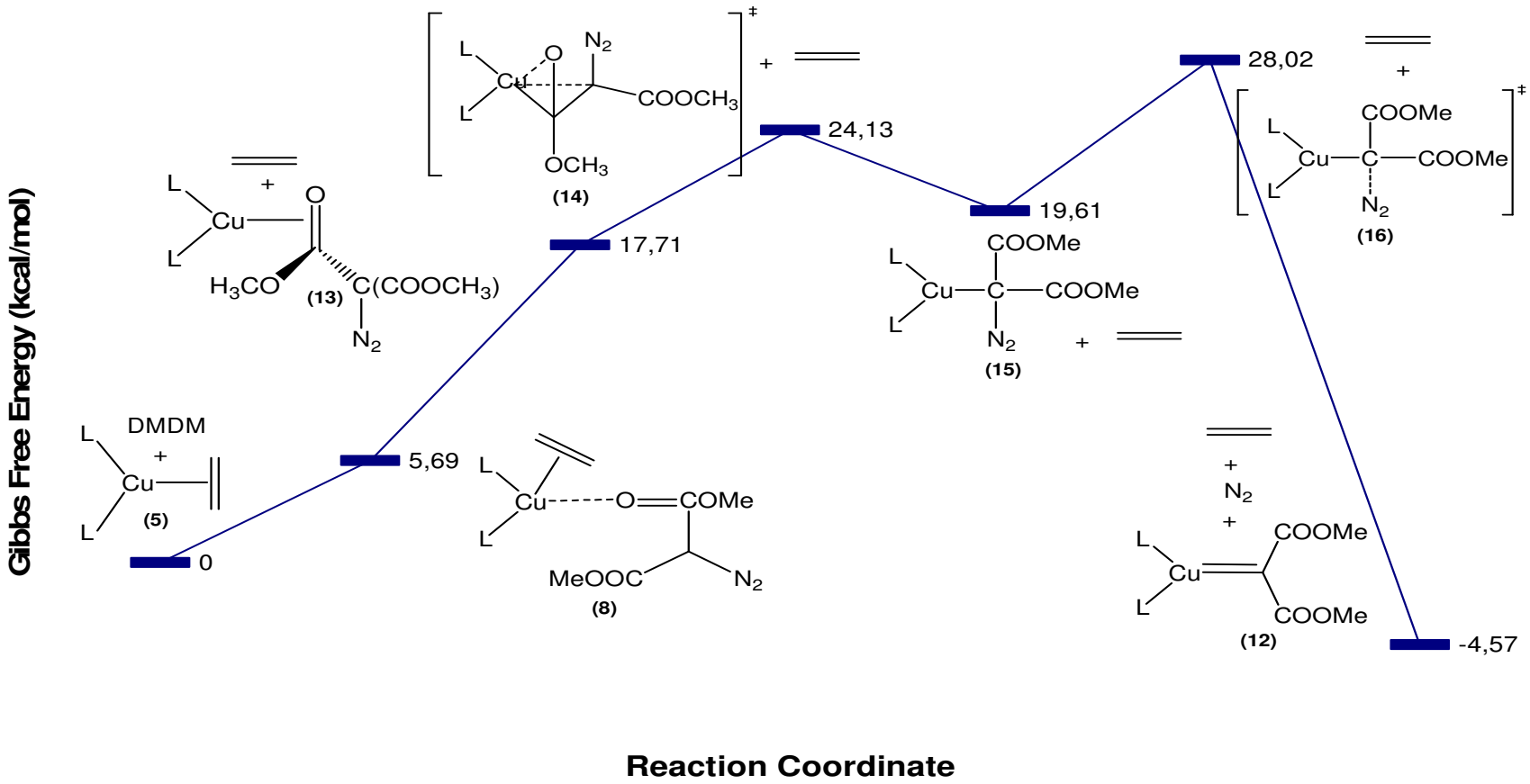

Scheme 4.2 : Mechanism **2**:Olefin Non-Assisted

4.1.3 Mechanism 3

This mechanism differs from Fraile et al. system from having a more detailed pathway from copper-alkene (**8**) to copper-diazo (**13**) transformation (Scheme **4.3**). Reaction sequence starts with catalyst-ethylene via associative displacement, and then the structure **8** is formed subsequently as in the mechanism of Fraile et al. However, after κO (**8**) complex formation, N_2 extrusion step does not occur. Instead, N is binded to copper to produce κO-N chelate complex. In the mechanism suggested by Straub et al., as the coordination of nitrogen to copper takes place, alkene is lost by the system simultaneously. However, analogous transition state could not be located for this system. Instead, κO-N and alkene loss take place in a step-wise manner with our system. In κN binding transition state **17** (Figure **4.11**), Cu coordinated more strongly to the carbonyl oxygen such that the 2.434 Å distance of Cu-O in **8** decreases to 2.162 Å in transition state **17**. At the same time, N coordination starts to occur which further weaken Cu's coordination to its ligand and alkene. This is reflected in Cu-C_{alkene} (1.943 Å and 1.939 Å in **8** and 1.988 Å and 1.971 Å in **17**) and Cu-O_{ligand} lengthenings (one of the Cu-O_{ligand} bond is 1.926 Å in **8** and 2.073 Å in **18**).

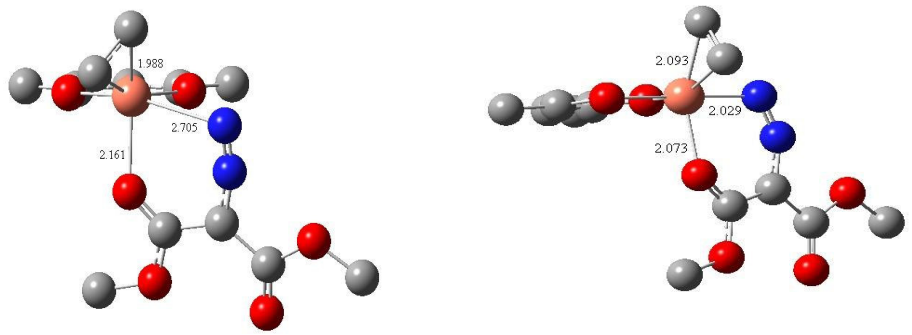

Figure 4.11 : 3-Dimensional Geometrical Structures of **17** and **18** (B3LYP/6-31G*)

Afterwards, alkene loss transition state **19** (Figure **4.12**) takes place and this process requires relatively small Gibbs free energy of 1.67 kcal/mol. Additionally, the energy values of alkene loss transtition state (**19**) and nitrogen binding transition (**17**) state are quite close to each other; 13.32 and 13.59 kcal/mol, respectively which can be interpreted that nitrogen binding and alkene loss happen simultaneously. According to kinetic studies on copper-alkene complexes, increase in ethene concentration resulted in rate-retardation [17]. This result has been interpreted by an existence of

equilibrium between catalyst-ethylene and catalyst-diazo complexes. The calculations on our system are in accordance with the kinetic studies such that the energy of **20** and **8** are close to each other, indicative of a pre-equilibrium before N_2 extrusion.

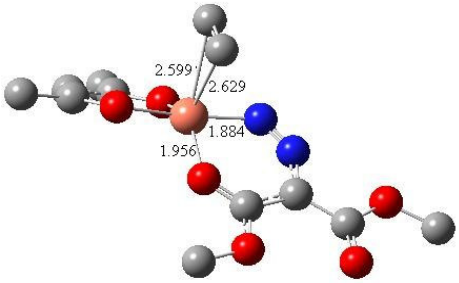

Figure 4.12 : 3-Dimensional Geometrical Structure of **19** (B3LYP/6-31G*)

Alkene loss leads to the intermediate **20** (Figure **4.13**) whose analogous structure has been determined by x-ray crystallography on an another Cu(I) catalyst with diazophenanthrone [45]. The Cu in **20** is almost square planar as observed in x-ray data of analogous structure from literature. Although this complex was emphasized as dead end in the work of Fraile et al., Straub et al. accomplished to carry on the mechanism from this structure **20** successfully. Moreover, same results are found in this study. Energetically, formation of catalyst-diazo intermediate is exothermic by 9.16 kcal/mol and structure **8** and catalyst-diazo intermediate have nearly the same relative Gibbs free energies 5.69 and 4.43 kcal/mol, respectively. Subsequently, Cu-N bond breaking transition state **21** (Figure **4.13**) takes place with a Gibbs free energy barrier of 23.58 kcal/mol. In this structure, Cu loses its coordination with N and compensates its loss by coordinating to π electron of carbonyl bond. In transition state **21**, the Cu-O_{DMDM} bond decreases from 1.888 Å to 1.858 Å. This reaction has the highest barrier in this mechanism.

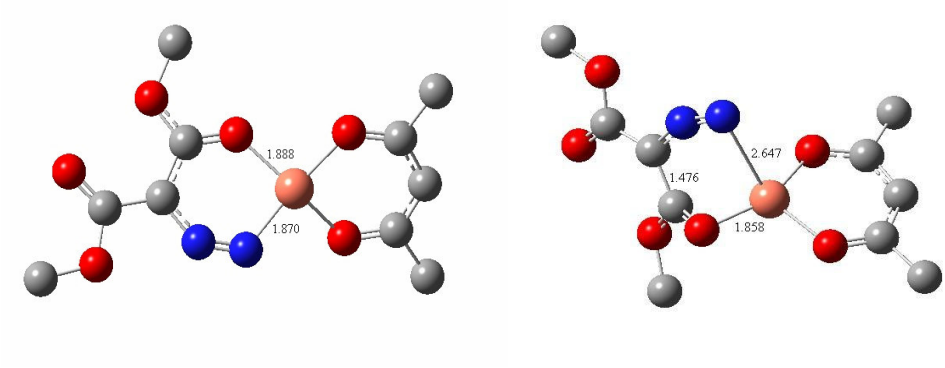

Figure 4.13 : 3-Dimensional Geometrical Structures of **20** and **21** (B3LYP/6-31G*)

After structure **13** is obtained, it undergoes olefin non-assisted N_2 extrusion step as in mechanism **2**. The copper-carbene complex is obtained through this sequence of reactions.

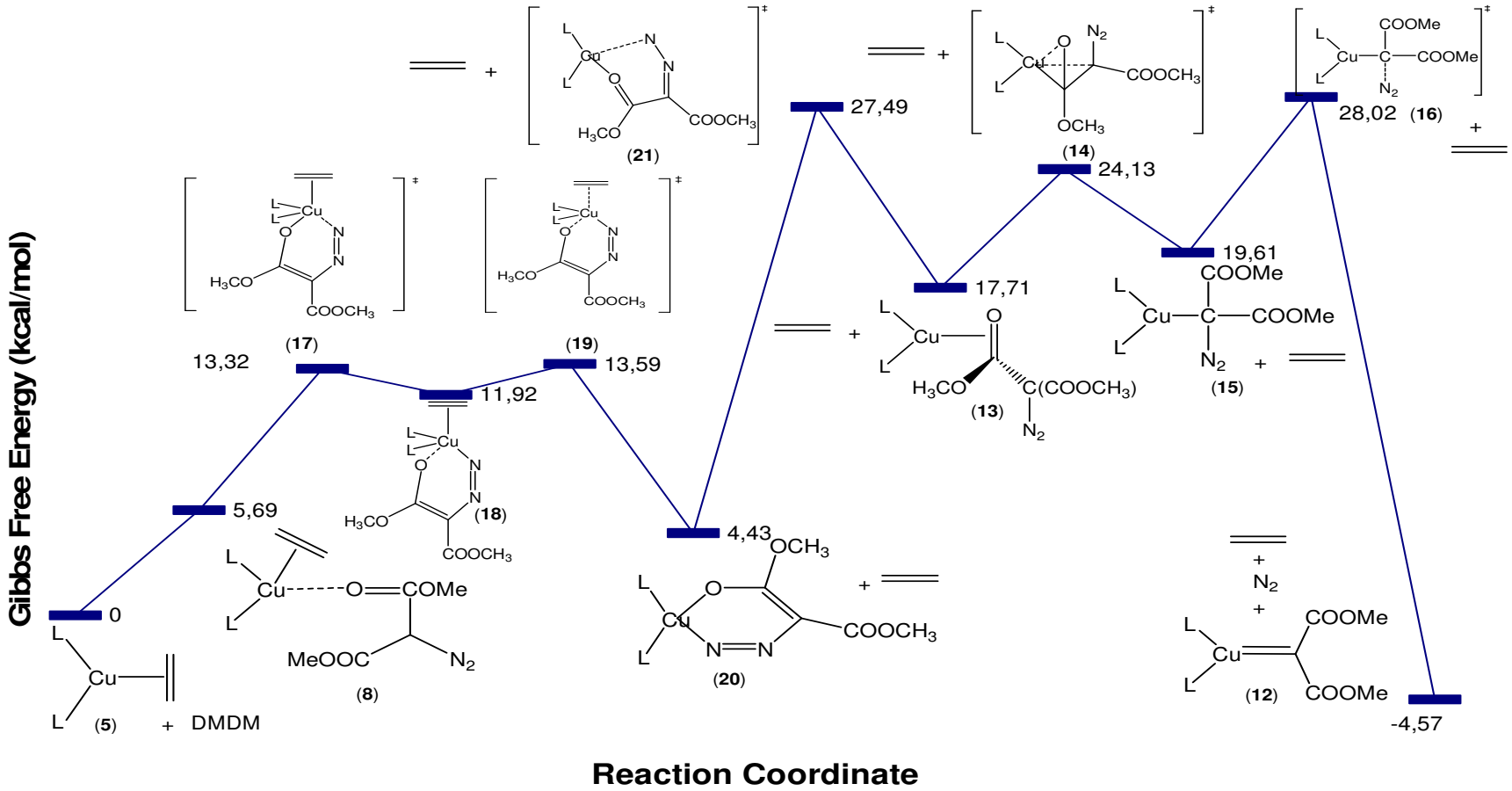

Scheme 4.3 : Mechanism **3**

4.2 Cyclopropanation Stage

When the copper-carbene formation stage is completed, then cyclopropanation takes place. For cyclopropanation two mechanisms; 3-centered and 4-centered (Scheme **1.3**) are possible. The 3 centered pathway (Scheme **4.4**) starts with transition state structure **22** (Figure **4.14).** Copper-carbene is a highly active intermediate because of its electrophilic character, thus it is inserted to the olefin molecule by way of the 3 centered pathway with producing metallocyclobutane stucture **23** (Figure **4.14**) in contrast to Fraile et al. mechanism. Geometrically, Cu-$C_{carbene}$ bond of structure **22** is 1.811 Å which is longer than the copper-carbene distance (1.770 Å). As the ethene molecule approaches to the copper-carbene system, metal loses its coordination to carbene C and further forms bonds to alkene with distances of 2.531 Å and 2.190 Å. This shows that the copper-carbene bond is weakened in structure **22.** The transition state **22** is activated with 9.7 kcal/mol of Gibbs free energy barrier. Although the mechanism is 3-centered, a metallocyclobutane molecule is formed which is supported by IRC studies due to the coordinative unsaturation of copper fragment and this observation is consisted with the results of Straub et al. results. In metallocyclobutane intermediate **23**, the Cu-$C_{carbene}$ bond length increased to1.940 Å where it also binded to alkene with a distance of 1.911 Å and it has a planar 4-membered ring. The C_{alkene}-C_{alkene} bond length increased to 1.510 Å since it has lost its double bond character. This reaction is highly exothermic.

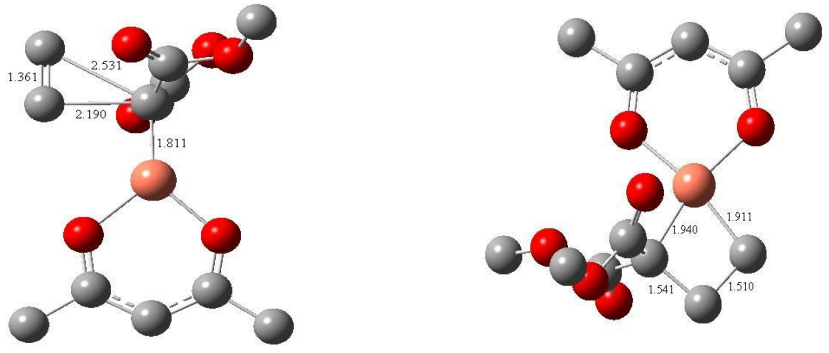

Figure 4.14 : 3-Dimensional Geometrical Structures of **22** and **23** (B3LYP/6-31G*)

As the cyclopropanation takes place through transition state **24** (Figure **4.15**) and catalyst intends to leave the system, it interacts with the lone-pairs of carbonyl oxygen at a distance of 1.862 Å. The interaction of Cu with the lone-pairs of oxygen

prevents coordinative unsaturation of Cu center. The Cu-C_{alkene} and Cu-$C_{carbene}$ bond lengths extended to 2.404 Å and 2.182 Å in transition state **24** (Figure **4.15**), respectively and the C atoms are close to form cyclopropane with a C_{alkene}-$C_{carbene}$ distance of 1.581 Å. Energetically, 15.74 kcal/mol of Gibbs free energy required for activation. The product of this transition state is structure **25** (Figure **4.15**). The carbonyl group is bonded to copper fragment. While Cu-C bond is 1.968 Å, Cu-O bond is 1.889 Å and C-O bond 1.279 Å. Gibbs free energy is decreased to -35.80 kcal/mol. Afterwards, the carbonyl carbon is detached from copper atom without a transition state (**26**). Because of the coordination lack of copper, Gibbs free energy is increased highly about 11 kcal/mol. There is an interaction between lone pairs of carbonyl oxygen and copper. Gibbs free energy is increased to -24.42 kcal/mol. The active catalyst further detached from the system and final product cyclopropane is obtained.

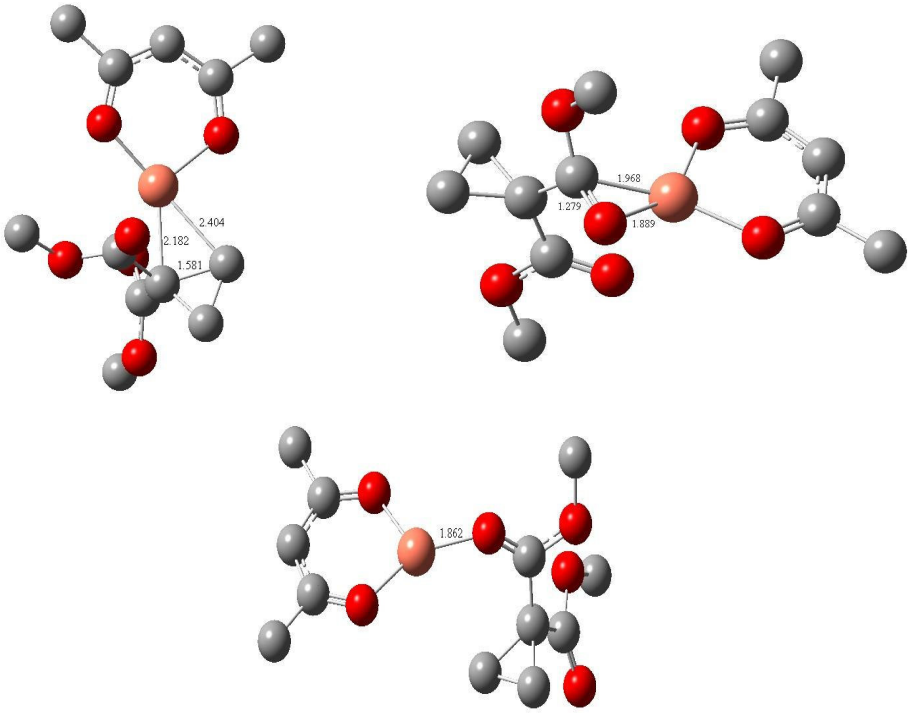

Figure 4.15 : 3-Dimensional Geometrical Structures of **24**, **25** and **26** (B3LYP/6-31G*)

Finally, the cyclopropane derivative structures **27a** and **27b** are formed after structure **25** through a barrierless process. The compound is in cis conformer **27a** whereas trans conformer of diazo compound **2** is starting species. However, energy difference between trans **27b** and cis **27a** conformers of final product is small by 1

kcal/mol which is attributed to easiness of rotation about single bond. C-C bond lengths in cyclopropyl group are 1.530 Å and in acetate group are 1.501 Å.

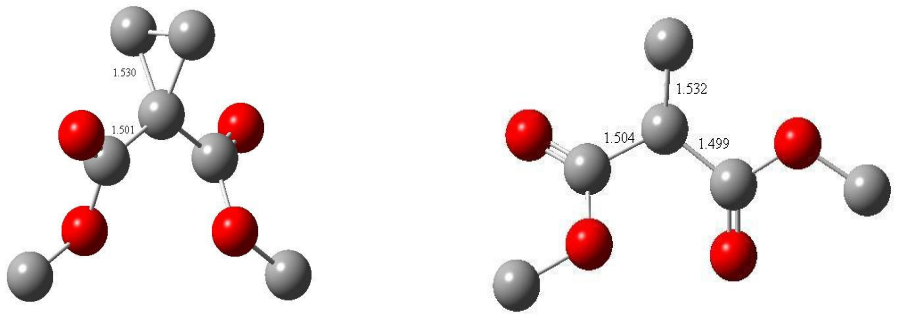

Figure 4.16 : 3-Dimensional Geometrical Structures of **27a** and **27b** (B3LYP/6-31G*)

On the other hand, 4-membered pathway was tried to obtain cyclopropanation from copper-carbene structure **12**. A 4-centered transition state could be located however, the IRC calculations indicated that the reactant of the 4-centered cyclopropanation stage is **10**, where alkene is complexed to Cu-carbene system. This result suggests that cyclopropanation may proceed before formation of copper carbene (**12**). However, this 4-centered pathway has been omitted for two reasons; first, carbene formation has been proven by x-ray crystallography on an analogous system. Secondly, once structure **10** forms it will resist cyclopropanation through a 4 membered transition state since alkene loss as in mechanism **1** is energetically favored.

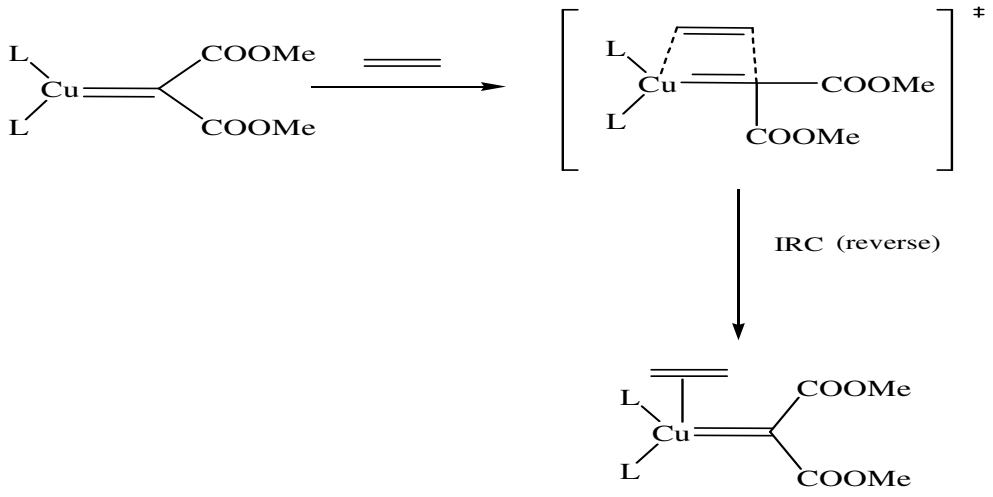

Figure 4.17 : The 4-membered Transition State and Its IRC Result

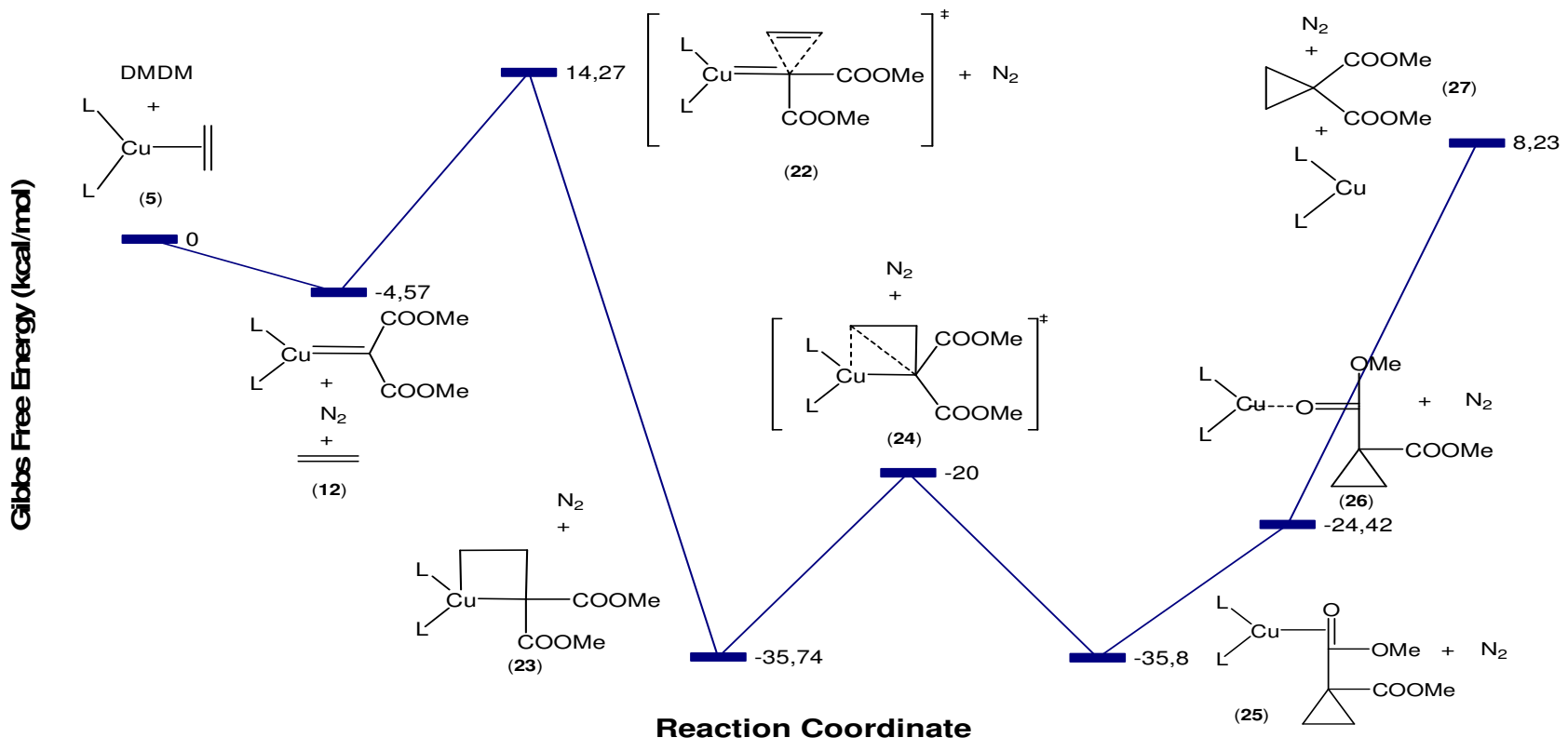

Scheme 4.4 : Cyclopropanation Stage

In mechanism 1 we have also questioned the possibility of cyclopropanation before carbene formation. In mechanism 1, one of the olefinic carbon atoms in structure **10** can detach copper and bind to the carbon that is bonded to Cu which produces a metallocyclobutane intermediate leading to cyclopropane (**28**). However this process requires 3.6 kcal/mol of higher energy than alkene loss does. Moreover, this process does not lead to a metal-carbene formation, whereas the existence of metal-carbene formation was proved by Straub and Hofmann in their copper catalyzed cyclopropanation reaction [6]. Thus this alternative step can be eliminated.

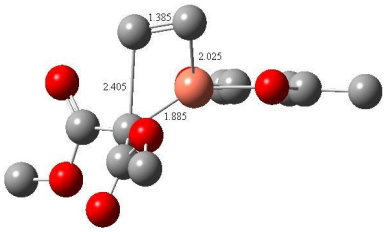

Figure 4.18 : 3-Dimensional Geometrical Structure of **28** (B3LYP/6-31G*)

Another alternative way of cyclopropanation can be through double alkene complexation to the active catalyst. This mechanism starts with structure **5** and then structure **10** forms through **8** and **9** as in mechanism **1**. At this point, a second alkene molecule approaches the carbon atom bonded to copper via transition state structure **29** shown in Figure **4.19**

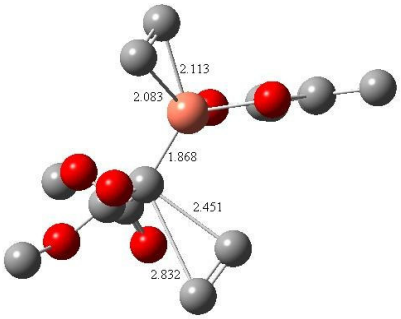

Figure 4.19 : 3-Dimensional Geometrical Structure of Complexation of Double Alkene (**29**) (B3LYP/6-31G*)

In this structure Cu-C_{DMDM} bond is extended to 1.868 Å from 1.843 Å. Meanwhile, Cu-C_{alkene} bonds shrink to 2.083 Å and 2.113 Å because of the increased coordination of Cu DMDM moiety. Forming C_{DMDM}-C_{alkene} bonds are 2.832 Å and 2.451 Å. Energetically, 17.62 kcal/mol Gibbs free energy is required for activation of this transition state structure. This amount of Gibbs free energy makes the mechanism unfavorable because 2.01 kcal/mol Gibbs free energy is sufficient for alkene extrusion (Figure **4.20**). Additionally, this mechanism does not have a copper-carbene complex structure. Thus, it can be concluded that cyclopropanation does not take place through this mechanism

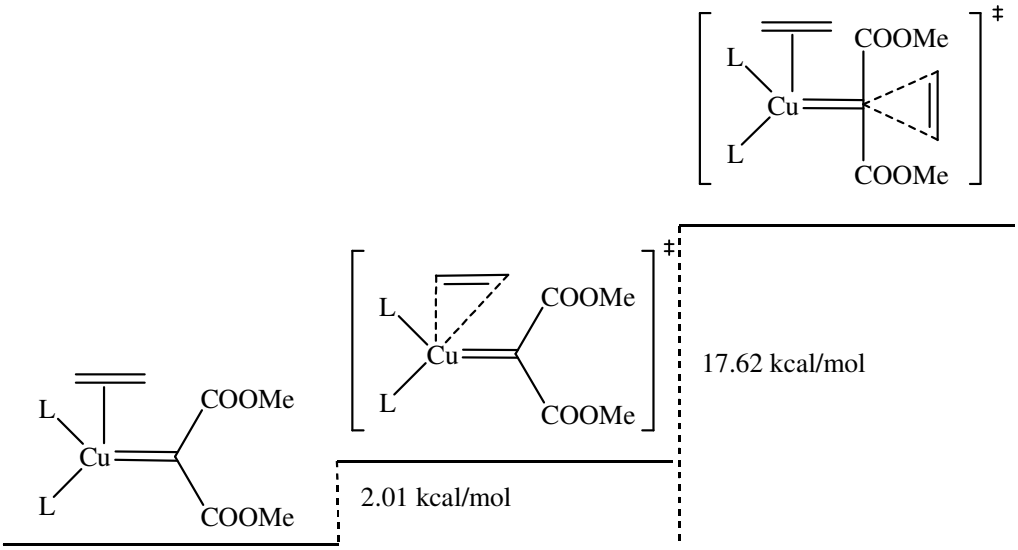

Figure 4.20 : Energy Differences of Structures **10**, **11** and **29** (B3LYP/6-31G*)

5. CONCLUSION

In this study, the mechanism of copper-catalyzed decomposition of dimethyldiazomalonate and cyclopropanation with ethene as substrate has been investigated by the Density Functional Theory, B3LYP/6-31G* basis set.

It is known from literature that different types of diazo compounds and different catalysts show variations in carbene formation and cyclopropanation mechanisms. Thus, it is an important task to understand the way a catalyst acts in the reaction. For this purpose, the possible mechanisms leading first to copper-carbene (Scheme **1.1** and Scheme **1.2**) then to cyclopropane (Scheme **1.3**) have been investigated.

The calculations for this system indicate that the associative displacement is more favorable than the dissociative by a much lower energy requirement (Figure **4.4**). This result is in agreement with other theoretical studies on other copper-catalyzed cylopropanation reactions [14,15].

Among the possible mechanisms considered in this study, mechanism **3** is found to be a more preferable pathway thermodynamically for carbene formation. The reacting species, **5** and **DMDM,** form structure **8** in each pathway. After **8**, there are three possibilities. If the alkene leaves the system and the complex undergoes an N_2 extrusion as in mechanism 2, the forming product (**15**) is at a relative energy of 19.61 kcal/mol (Scheme **4.2**). One step reaction from **8** to **13** requires the lowest barrier of 12.02 kcal/mol (Mechanism 2). Olefin assisted N_2 extrusion, starting from structure **8** according to mechanism **1**, is even higher than this value (24.18 kcal/mol) from Scheme **4.1**). However, binding through κN in transition structure **17** according to mechanism **3** requires the lowest barrier (7.63 kcal/mol). These barriers indicate that the Cu---O complexed structure (**8**) will undergo carbene formation through mechanism **3** and excludes mechanism **1** and **2** as possible pathways.

The preferred pathway mechanism **3** is a feasible pathway because it is in accordance with experimental studies on analogous systems. In a copper catalyzed cyclopropanation study a κN,O strcuture, similar to **20**, has been detected by x-ray

crystallography. The pre-equilibrium between copper-alkene and copper-diazo complex, evidenced from kinetic studies, is also present in this mechanism.

Cyclopropanation without carbene formation is considered for this system, however, these processes via single-alkene or double alkene paths are found to be energetically unfavorable. Cyclopropanation via copper-carbenes can take place via two possible mechanisms: transition state structures (Scheme **1.3**). For this system, DFT calculations showed that a mixture of these paths is possible. The 4-centered transition structure following carbene is found to be at a higher energy than the 3-centered transition structure. Additionally, IRC calculations on the 4-centered transition structure revealed alkene-complexed copper-carbene structure instead of free carbene. IRC calculations on 3-centered transition structure gave unexpectedly metallacyclobutane as product, which further transformed into cyclopropane. Moreover, contrary to literature, the cyclopropanation takes place in step-wise manner instead of concerted manner.

The overall picture shows that metal-carbene forms through mechanism **3** and followed by a 3-centered transition structure which gives a 4-membered ring intermediate and this indicates that coordinated saturation of transition metal fragment in catalyst has influence on the fate of the mechanism. In the whole mechanism, the rate determining step is in carbene formation, which is in accordance with the previous experimental and theoretical findings.

REFERENCES

[1] **Doyle, M., McKervey, Anthony., and Ye, Tao.,** 1998. Modern Catalytic Methods for Organic Synthesis with Diazo Compounds, John Wiley & Sons, Inc, pp 66-177, New York

[2] **Norrby, Per-ola., and et al.,** 2002. On the Mechanism of the Copper-Catalyzed Cyclopropanation Reaction, *Chem. Eur. Journal*, 8, No:1, 177-184.

[3] **Suenobu, Katsuhiro. and et al.,** 2004**.** Reaction Pathway and Stereoselectivity of Asymmetric Synthesis of Chrysanthemate with the Aratani C_1-Symmetric Salicylaldimine-Copper Catalyst, *Journal of American Chemical Society*, 126, 7271-7280

[4] **Bühl, M., U, Lüning. and et al.,** 2001. On the Mechanism and Stereoselectivity of the Copper(I)-Catalyzed Cyclopropanation of Olefins- A combined Experimental and Density Functional Study, *European Journal of Organic Chemistry*, 2151-2160.

[5] **Kirmse, W.,** 2003. Copper Carbene Complexes: Advanced Catalysts, New Insights, *Angew. Chem. Int. Ed*, 42, No: 10

[6] **Straub, B.F. and Hofmann, P.,** 2001. Copper(I) Carbenes: The Synthesis of Active Intermediates in Copper-Catalyzed Cyclopropanation, *Angew. Chem. Int. Ed*, 40, No: 7

[7] **Smith, D.A., Reynolds, D. and Woo, L.,** 1993. Cyclopropanation Catalyzed by Osmium Porphyrin Complexes, *Journal of American Chemical Society*, 155, 2511-2513

[8] **Park, S.B., Sokata, N. and Nishiyama. H,** 1996. Aryloxycarbonylcarbene Complexes of Bis(oxazolinyl) pyridineruthenium as Active Intrmediates in Asymmetric Catalytic Cyclopropanations, *Chemistry-A European Journal*, 2, 303-306.

[9] **Pfaltz, A. and Yamamoto, H.,** 1999. Cyclopropanation and C-H insertion Cu. In Comperehensive Asymmetric Catalysis, Springer-Verlag, Vol.2, pp 513-538, Berlin

[10] **Cornejo, A. and et al.,** 2005. Computational Mechanistic Studies on Enantioselective pybox-Ruthenium-Catalyzed Cyclopropanation Reactions, *Organometallics*, 24, 3448-3457

[11] **Pfaltz, A., and Yamamoto, H.,** 1999. Cyclopropanation and C-H insertion Cu. In Comperehensive Asymmetric Catalysis, Springer-Verlag, Vol.2, pp 539-580, Berlin

[12] **Nozaki, H., Moriuti, S., Takaya, H., and Noyori, R.,** 1966. Asymmetric Induction in Carbenoid Reaction by Means of a Disymmetric Copper Chelate, *Tetrahedron Letters*, 5239-5244.

[13] **Aratani, T.,** 1985. Catalytic Aymmetric Synthesis Of Cyclopropane-Carboxylic acids: An Application of Chiral Copper Carbenoid Reaction, *Pure Appl. Chem, 57,* 1839-1844.

[14] **Fraile, M. and et al.,** 2001. Theoretical Insight into the Mechanism of Copper-Catalyzed Cyclopropanation Reactions. Implications for Enantioselective Catalysis, *Journal of American Chemical Society*, 123, 7616-7625.

[15] **Straub, B. and et al.,** 2003. Mechanism of Copper(I)-Catalyzed Cyclopropanation: a DFT Study Calibrated with Copper(I) Alkene Complexes, *Journal of Organometallic Chemistry,* 684*,* 124-143.

[16] **Salomon, R. G. and Kochi, J. K.,** 1973. Copper(I) Catalysis in Cyclopropanations with Diazo Compounds. Role of Olefin Coordination, *Journal of American Chemical Society,* 95, 3300-3310.

[17] **Diaz-Requejo, M.M., Nicasio, M.C. and Perez, P.J**., 1998. BpCu-Catalyzed Cyclopropanation of Olefins: A Simple System That Operates under Homogeneous and Heterogeneous Conditions (Bp= Dihydridobis(pyrazolyl)borate), *Organometallics*, 17, 3051–3057.

[18] **Talınlı, N., Karliğa, B. and Anaç, O.,** 2000. Investigations on the Reactions of a Carbonylcarbene with Substituted 1,3-Dioxepins, *Helvetica Chimica Acta,* 83, 966–971

[19] **Tüzün, N.Ş.,** 2002. Analysis of the Radical Polymerizability of Diallyl Monomers, *PhD Thesis,* Boğaziçi University.

[20] **Atkins. P. and Friedman R.,** 2005. Molecular Quantum Mechanics, Oxford University Press, Fourth Edition, pp 287-289, New York.

[21] **Hohenberg, P. and Kohn, W.,**1964. Inhomogeneous Electron Gas**,** *Phys. Rev.,* 136, B864 - B871

[22] **Hohenberg, P. and Kohn, W.,**1965. Self-Consistent Equations Including Exchange and Correlation Effects, *Phys. Rev*. 140, A1133 - A1138.

[23] **Salahub, D. R. and Zerner, M. C.,** 1989. *The Challenge of d and f Electrons*, ACS, Washington, D.C.

[24] **Parr, R. G. and Yang, W.,** 1989. *Density-Functional Theory of Atoms and Molecules*, Oxford Univ. Press, Oxford.

[25] **Roothan, C. C. J.,** 1951. New Developments in Molecular Orbital Theory, *Rev. Mod. Phys*, 23, 69 – 89.

[26] **Pople, J. A. and Nesbet, R. K.,** 1954. Self-Consistent Orbitals for Radicals, ***J.*** *Chem. Phys.* 22, 571.

[27] **McWeeny, R. and Dierksen, G**., 1968. Self-Consistent Perturbation Theory. II. *J. Chem. Phys.* 49**,** 4852

[28] **Becke, A.D.,** 1993. Density-functional thermochemistry. III The Role of Exact Exchange., *J. Chem. Phys,* 98, 5648.

[29] **Jensen, F.,** 1999. Introduction to Computational Chemistry, John Wiley and Sons, pp 150-350, England

[30] **Gonzalez, C. and Schlegel, H.B.,** 1989. An Improved Algorithm for Reaction Path Fallowing, *J. Chem. Phys.* 90, 2154

[31] **Gonzalez, C. and Schlegel, H.B.,** 1990. Reaction Path Following in mass-Weighted Internal Coordinates, *J. Phys. Che..* 94, 5523

[32] http://www.iupac.org/reports/1999/7110minkin/i.html (2007)

[33] **Carpenter, J.E. and Weinhold** F., 1988. Analysis of the Geometry of the Hydroxymethyl Radical by the "Different Hybrids for Different Spins" Natural Bond Orbital Procedure, *THEOCHEM,* 169, 41.

[34] **Carpenter, J.E.,** 1987. PhD thesis, University of Wisconsin, Madison, WI,.

[35] **Foster, J.P. and Weinhold, F**., 1980. Natural Hybrid Orbitals, *Journal of American Chemical Society,* 102, 7211-7218.

[36] **Reed, A.E. and Weinhold, F**., 1983. Natural Hybrid Orbital Analysis Of Near Hartree-Fock Water Dimer , *J. Chem. Phys.* 78, 4066-4073.

[37] **Reed, A. E. and Weinhold, F.,** 1983. Natural Localized Molecular-Orbitals, *Journal of Chemical Physics*, 83, 1736-1740

[38] **Reed, A. E., Weihstock, R. B. and Weinhold, F.,** 1985. Natural-Population Analysis, *Journal of Chemical Physics,* 83, 735-746

[39] **Carpenter, A. E. and Weinhold, F.,** 1988. *Plenum*, 227, 1988.

[40] **Reed, A. E., Curtiss, L. A. and Weinhold, F**., 1988. Intermolecular Interactions from a Natural Bond Orbital, Donor-Acceptor Viewpoint, *Journal of Chem. Rev. (Washington D.C.),* 88, 899-926**.**

[41] **Frisch, M. J., Trucks, G. W., Schlegel, H. B., Scuseria, G. E., Robb, M. A., Cheeseman, J. R., Montgomery, J. A., Vreven, Jr., T., Kudin, K. N., Burant, J. C., Millam, J. M., Iyengar, S. S., Tomasi, J., Barone, V., Mennucci, B., Cossi, M., Scalmani, G., Rega, N., Petersson, G. A., Nakatsuji, H., Hada, M., Ehara, M., Toyota, K., Fukuda, R., Hasegawa, J., Ishida, M., Nakajima, T., Honda, Y., Kitao, O., Nakai, H., Klene, M., Li, X., Knox, J. E., Hratchian, H. P., Cross, J. B., Adamo, C., Jaramillo, Gomperts, R., Stratmann, R. E., Yazyev, O., Austin, A. J., Cammi, R., Pomelli, C., Ochterski, J. W., Ayala, P. Y, Morokuma, K., Voth, G. A., Salvador, P., Dannenberg, J. J., Zakrzewski, V. G., Dapprich, S., Daniels, A. D., Strain, M. C., Farkas, O., Malick, D. K., Rabuck, A. D., Raghavachari, K., Foresman, J. B., Ortiz, J. V., Cui, Baboul, A. G. , Clifford, S., Cioslowski, J., Stefanov, B. B., Liu, G., Liashenko, A., Piskorz, P., Komaromi, I.,RMartin, . L., Fox, D. J., Keith, T., Al-Laham, M. A., Peng, C. Y., Nanayakkara, A., Challacombe, M.,Gill, P. M. W., Johnson, B., Chen, W.,Wong, M. W., Gonzalez, C. and Pople J. A.,** 2004. Gaussian 03, Revision C.02, *Gaussian, Inc*., Wallingford CT.

[42] **Cornejo, A. and et al.,** 2005. Computational Mechanistic Studies on Enantioselective pybox-Ruthenium-Catalyzed Cyclopropanation Reactions, Organometallics*.,* 24, 3448-3457.

[43] **Straub, B.F.,** 2002, Pd(0) Mechanism of Palladium-Catalyzed Cyclopropanation of Alkenes by CH_2N_2: A DFT Study, 124(47); 14195-14201

[44] **Raubenheimer, H. G., Cronje, S. and Olivier, P. J**., 1995, Synthesis and Characterization of Mono(carbene) Complexes of Copper and Crystal Structure of a Linear Thiazolinylidene Compound, *J. Chem. Soc., Dalton Trans.*, 1995, (2),313-316

[45] **Straub, B. F., Rominger, F. and Hofmann, P**., 2000, A Fluxional -Carbonyl Diazoalkane Complex of Copper Relevant to Catalytic Cyclopropanation, *Organometallics,* 19(21), 4305-4309

APPENDIX

	Electronic Energy (Hartree)	Gibbs Free Energy (Hartree)	Relative Gibbs Free Energy (kcal/mol)
Structure **1**	-1985.49552358	-1985.417727	-
Structure **2**	-604.50022824	-604.418867	-
Structure **3**	-604.50016194	-604.418539	-
Structure **4**	-604.49924558	-604.417725	-
Structure **5**	-2064.16622492	-2064.037314	0
Structure **6**	-2142.75689154	-2142.580350	9.23
Structure **7**	-2668.67261616	-2668.445813	6.50
Structure **8**	-2668.67728080	-2668.447103	5.69
Structure **9**	-2668.63463745	-2668.408568	29.87
Structure **10**	-2559.13144819	-2558.909936	5.81
Structure **11**	-2559.12943047	-2558.906727	7.82
Structure **12**	-2480.53939276	-2480.368728	-4.57
Structure **13**	-2590.04974118	-2589.870193	17.71
Structure **14**	-2590.04030997	-2589.859967	24.13
Structure **15**	-2590.04643986	-2589.867165	19.61
Structure **16**	-2590.03022759	-2589.853767	28.02
Structure **17**	-2668.66357868	-2668.434939	13.32
Structure **18**	-2668.66876950	-2668.437185	11.92
Structure **19**	-2668.66409212	-2668.434522	13.59
Structure **20**	-2668.07450646	-2589.891356	4.43
Structure **21**	-2668.03445134	-2589.854616	27.49
Structure **22**	-2559.11993423	-2558.896450	14.27
Structure **23**	-2559.20491228	-2558.976162	-35.74
Structure **24**	-2559.18095331	-2558.951058	-20.00
Structure **25**	-2559.20616496	-2558.976255	-35.80

Structure **26**	-2559.18518239	-2558.958115	-24.42
Structure **27a**	-574.64593904	-573.516184	-8.23
Structure **28**	-2559.12496044	-2558.900996	17.19
Structure **29**	-2637.71064215	-2637.439625	23.43
Ethene	-78.58745824	-78.557760	-
N_2	-109.52412907	-109.536980	-

BIOGRAPHY

Cihan ÖZEN was born in 1982, İstanbul. He graduated from İsmail Rüştü Olcay High School - İstanbul in 1999. He started his undergraduate education in Abant İzzet Baysal University, Chemistry Department, and obtained BSc. Degree at Chemistry Department in January, 2005. Immediately after his graduation, he attended in İstanbul Technical University, Chemistry, where he prepared hereby master thesis.